AD-A263 496

WL-TR-92-2097

PULSE MITIGATION AND HEAT TRANSFER
ENHANCEMENT TECHNIQUES

VOL 3 - LIQUID SODIUM HEAT TRANSFER FACILITY
AND TRANSIENT RESPONSE OF SODIUM HEAT PIPE TO
PULSE FORWARD AND REVERSE HEAT LOAD

L.C. Chow
O.J. Hahn
H.X. Nguyen
University of Kentucky
Department of Mechanical Engineering
Lexington, KY 40506-0046

AUG 1992

FINAL REPORT FOR 07/01/87 - 07/31/92

DTIC
ELECTE
MAY 0 3 1993
S B D

93-09310

AERO PROPULSION AND POWER DIRECTORATE
WRIGHT LABORATORY
AIR FORCE MATERIEL COMMAND
WRIGHT PATTERSON AFB OH 45433-6563

NOTICE

When Government drawings, specifications, or other data are used for any purpose other than in connection with a definitely Government-related procurement, the United States Government incurs no responsibility or any obligation whatsoever. The fact that the government may have formulated or in any way supplied the said drawings, specifications, or other data, is not to be regarded by implication, or otherwise in any manner construed, as licensing the holder, or any other person or corporation; or as conveying any rights or permission to manufacture, use, or sell any patented invention that may in any way be related thereto.

This report is releasable to the National Technical Information Service (NTIS). At NTIS, it will be available to the general public, including foreign nations.

This technical report has been reviewed and is approved for publication.

MICHAEL J MORGAN
Project Engineer

JERRY E. BEAM, Chief
Thermal Technology Section

MICHAEL D. BRAYDICH, Lt Col, USAF
Deputy Chief
Aerospace Power Division
Aero Propulsion & Power Directorate

If your address has changed, if you wish to be removed from our mailing list, or if the addressee is no longer employed by your organization please notify WL/POOS , WPAFB, OH 45433- 6563 to help us maintain a current mailing list.

Copies of this report should not be returned unless return is required by security considerations, contractual obligations, or notice on a specific document.

WL-TR-92-2097

PULSE MITIGATION AND HEAT TRANSFER
ENHANCEMENT TECHNIQUES

VOL 3 - LIQUID SODIUM HEAT TRANSFER FACILITY
AND TRANSIENT RESPONSE OF SODIUM HEAT PIPE TO
PULSE FORWARD AND REVERSE HEAT LOAD

L.C. Chow
J.J. Hahn
H.X. Nguyen
University of Kentucky
Department of Mechanical Engineering
Lexington, KY 40506-0046

AUG 1992

FINAL REPORT FOR 07/01/87 - 07/31/92

APPROVED FOR PUBLIC RELEASE; DISTRIBUTION IS UNLIMITED.

NOTICE

When Government drawings, specifications, or other data are used for any purpose other than in connection with a definitely Government-related procurement, the United States Government incurs no responsibility or any obligation whatsoever. The fact that the government may have formulated or in any way supplied the said drawings, specifications, or other data, is not to be regarded by implication, or otherwise in any manner construed, as licensing the holder, or any other person or corporation; or as conveying any rights or permission to manufacture, use, or sell any patented invention that may in any way be related thereto.

This report is releasable to the National Technical Information Service (NTIS). At NTIS, it will be available to the general public, including foreign nations.

This technical report has been reviewed and is approved for publication.

MICHAEL J MORGAN
Project Engineer

JERRY E. BEAM , Chief
Thermal Technology Section

MICHAEL D. BRAYDICH, Lt Col, USAF
Deputy Chief
Aerospace Power Division
Aero Propulsion & Power Directorate

If your address has changed, if you wish to be removed from our mailing list, or if the addressee is no longer employed by your organization please notify WL/POOS , WPAFB, OH 45433- 6563 to help us maintain a current mailing list.

Copies of this report should not be returned unless return is required by security considerations, contractual obligations, or notice on a specific document.

REPORT DOCUMENTATION PAGE

1. AGENCY USE ONLY (Leave blank)	2. REPORT DATE	3. REPORT TYPE AND DATES COVERED	
	AUG 1992	FINAL	07/01/87--07/31/92

4. TITLE AND SUBTITLE PULSE MITIGATION AND HEAT TRANSFER ENHANCEMENT TECHNIQUES, Vol 3 - Liquid Sodium Heat Transfer Facility and Transient Response of Sodium Heat Pipe to Pulse Forward and Reverse Heat Load

6. AUTHOR(S) C. Chow
O.J. Hahn
H.X. Nguyen

5. FUNDING NUMBERS

C F33615-87-C-2777
PE 63218
PR D812
TA 00
WU 08

7. PERFORMING ORGANIZATION NAME(S) AND ADDRESS(ES)

University of Kentucky
Department of Mechanical Engineering
Lexington, KY 40506-0046

8. PERFORMING ORGANIZATION REPORT NUMBER

UK-ME-92-03

9. SPONSORING/MONITORING AGENCY NAME(S) AND ADDRESS(ES) AERO PROPULSION AND POWER DIRECTORATE
WRIGHT LABORATORY
AIR FORCE MATERIEL COMMAND
WRIGHT PATTERSON AFB OH 45433-6563
WL/POOS, Attn: MORGAN 513-2552922

10. SPONSORING/MONITORING AGENCY REPORT NUMBER

WL-TR-92-2097

11. SUPPLEMENTARY NOTES

12a. DISTRIBUTION/AVAILABILITY STATEMENT APPROVED FOR PUBLIC RELEASE; DISTRIBUTION IS UNLIMITED.

12b. DISTRIBUTION CODE

13. ABSTRACT (Maximum 200 words) This report presents the description of a liquid sodium heat transfer facility (sodium loop) constructed to support the study of transient response of heat pipes. The facility, consisting of the loop itself, a safety system, and a data acquisition system, can be safely operated over a wide range of temperature and sodium flow rate. The transient response of heat pipe to pulse heat load at the condenser section was experimentally investigated. A 0.457 m (18") long, screen wick, sodium heat pipe with 0.0127 m (0.5") outer diameter was tested under different heat loading conditions. Major finding was that the heat pipe reversed under a pulse heat load applied at the condenser. The time of reversal was approximately 15 to 25 seconds. The startup of heat pipe from frozen state was also studied. It was found that during startup process, at least part of the heat pipe was active. The active region extended gradually down to the end of the condenser until all working fluid in the heat pipe was molten.

14. SUBJECT TERMS SODIUM HEAT PIPE, SODIUM LOOP, TRANSIENT RESPONSE OF HEAT PIPES, PULSE HEAT LOAD

15. NUMBER OF PAGES 95

16. PRICE CODE

17. SECURITY CLASSIFICATION OF REPORT	18. SECURITY CLASSIFICATION OF THIS PAGE	19. SECURITY CLASSIFICATION OF ABSTRACT	20. LIMITATION OF ABSTRACT
UNCLASSIFIED	UNCLASSIFIED	UNCLASSIFIED	UL

ii

TABLE OF CONTENTS

iii

LIST OF ILLUSTRATIONS

LIST OF TABLES

1. INTRODUCTION

In future space platforms, it is envisioned that waste heat can be removed from a high temperature heat source through a closed sodium loop. The waste heat acquired by the sodium flow is rejected to space through a heat pipe radiator. One problem needed to be studied is the transient response of the coupled sodium loop/heat pipe radiator when subject to adverse thermal loading at the heat pipe radiator. Under an adverse condition, a pulse heat load can be applied to the condenser section of a heat pipe. This pulse heat load can raise the heat pipe temperature above the loop temperature causing the heat pipe to function in reverse mode. Thus instead of removing heat from the loop, the heat pipe actually transfers heat into the system.

A liquid sodium loop facility was constructed to support this research. The loop circulated liquid sodium at high temperature to a test cell where it flows over an inserted heat pipe. This provided a realistic thermal loading at the evaporator section of the heat pipe being tested. Although the idea of circulating working fluid within a loop was relatively simple, the high operational temperature and the extreme reactive and corrosive nature of sodium made the design of loop a challenging task.

The facility consisted of three major components: the sodium loop, the safety system, and the data acquisition system. Since the loop was designed to operate in wide range of temperature and flow rate, the controls of thermal power inputs and sodium flow rate are necessary. The safety system must be equipped with detector and sensor to take appropriate action in case of accidental fire. The data acquisition system provides a real-time measurement of the experimental data.

The research reported later in this report is an experimental investigation

of the transient response of heat pipe to pulse heat loading at the condenser section. Earlier, Tilton and Chow (1, 2) had conducted the experimental and theoretical investigations of the response of liquid metal heat pipe to an adverse thermal loading at the condenser. Their experiment, however, failed to illustrate a true reversal process since the evaporator was not subjected to a convective cooling/heating medium. The experiment described in this report was an attempt to show the reversal characteristic of a liquid metal heat pipe.

Three different types of thermal loading at the condenser were studied: 1. Condenser was fully heated; 2. Condenser was partially heated with the remaining insulated; 3. Condenser was partially heated with the remaining exposed to room air. The condenser heat input was obtained by sliding the cylindrical shell radiant heater over the end of the heat pipe condenser. The recorded data measurements included the external wall temperature distribution, both axially and radially, as a function of time. The inlet and outlet temperatures of the test cell were also recorded to allow the calculation of the amount of heat transferred by the heat pipe to (or from) the sodium loop.

2. LIQUID SODIUM SYSTEM

Sodium loop was designed and constructed to circulate liquid sodium at high temperature for testing purposes of heat pipes or other thermal devices. The loop was originally built by Mr. Paul Kreitz and its full descriptions can be found in Mr. Kreitz's thesis entitled Design and Construction of Liquid Metal Heat Transfer Facility. Due to some technical difficulties especially the carbon build-up in loop piping, the original loop had never been in operation. January 1990, the loop was rebuilt since every attempt to clear the clogged loop piping had failed. The new loop described in this report used the same concept as the original one; however, many parameters had been changed or added to simplify the loop operation, yet provided better control and safety.

2.1 SODIUM FLOW DESCPIPTIONS

About 12.25 Kg (27 lb) of sodium was stored in the loop. Upon activation, the electromagnetic pump moved the sodium upward through loop piping. At the bypass line, a portion of the sodium was diverted back to the pump entrance. The purpose of this bypass line was to provide better control of sodium temperature at the pump cell and sodium flow at the test section. With the bypass valve fully opened, approximately 55% of the flow can be diverted back. The remaining portion of the sodium flowed upward through two concentric-tube counter flow heat exchangers (economizer). Leaving the economizer, the sodium followed the test section line to the test cell. Here it flowed over the inserted heat pipe providing the necessary cooling or heating for testing purposes. From the test cell, sodium flowed into the surge tank. The sodium flow then exited through the bottom of the surge tank to a filter. From the

3

filter, sodium entered the economizer. Here the hot downward flow donated its thermal energy to the cooler upward flow. After leaving the economizer, the sodium flowed into a finned heat exchanger, or cooler, where it was cooled prior to returning to the pump cell. The cooler helped to maintain the pump cell within its operational temperature range. A schematic of sodium flow is shown in Figure 2.1.

2.2 SODIUM LOOP COMPONENTS

This section gives the descriptions of major components and devices used in the sodium loop.

2.2.1 COVER GAS SYSTEM: To prevent air from entering the system, a positive pressure must be maintained in the sodium loop; 99.999% pure nitrogen was used. The cover gas system allowed different pressures to be maintained in the surge and dump tanks during charging and draining of sodium. These pressures can be equalized or released by opening the proper valves. The cold traps help to capture sodium vapor in the event that gas pressure must be released. Figure 2.2 shows the schematic of loop cover gas system.

2.2.2 DUMP TANKS: Dump tanks served as a storage area for liquid sodium during changing, draining or when sodium level in the loop piping must be lowered. For the latter reason, dump tank location was the lowest point in the loop. There are two dump tanks in the sodium loop. Their dimensions are:
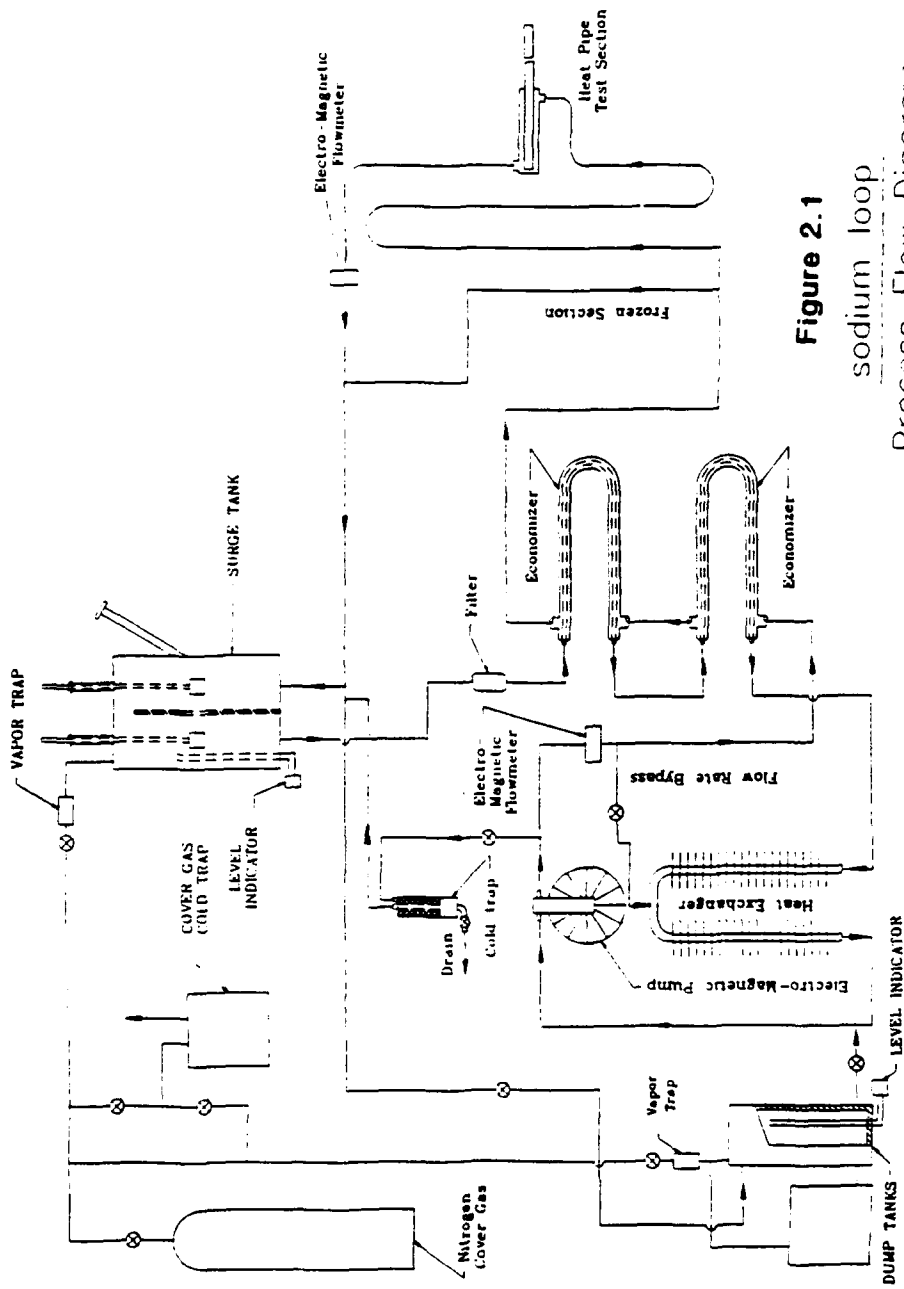
Figure 2.1

sodium loop
Process Flow Diagram

Symbols:

R	Regulator
⋈	Valves
P	Pressure Gage

Nitrogen Tank

Nitrogen Tank

Pressure Release Valves

Cold Trap

Cold Trap

Cold Trap

Sump

Surge Tank

Pressure Equalizing Valve

Dump Tank #1
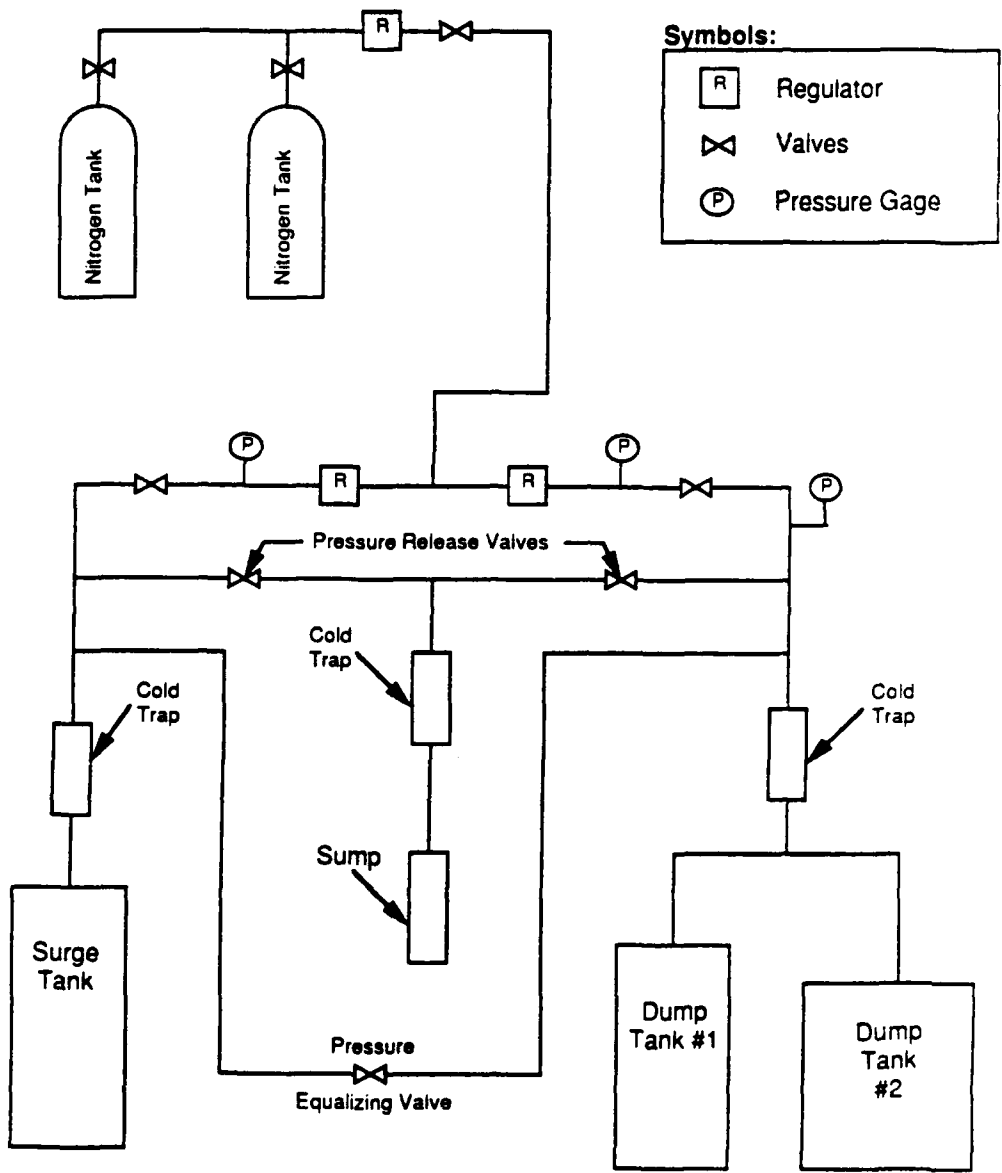
Dump Tank #2

Figure 2.2: Schematic of Cover Gas System

Dump tank #1: diameter: 0.222 m (8.75 in)

height: 0.584 m (23 in)

volume: 0.0224 m^3 (1368 in^3)

Dump tank #2: diameter: 0.314 m (12.375 in)

height: 0.289 m (11.375 in)

volume: 0.0227 m^3 (1383 in^3)

The two tanks were inter-connected. Since less sodium was used in the new loop (27 pounds compared to 100 pounds in the original loop) and to further reduce the amount of sodium needed, it was decided to use only dump tank #1. The connecting line was kept frozen thus sealed off the dump tank #2.

2.2.3 COLD TRAP: Impurities such as oxide, carbon, metals, hydrogen, etc., reduce the heat transfer capability of liquid sodium. Furthermore, they tend to enhance the corrosion or plugging of loop piping and vessels. The cold trap utilizes the positive temperature dependence of solubility (i.e., solubility decreased with decreasing temperature) to purify the sodium. As liquid sodium is cooled beyond the saturation temperature for a given impurity concentration, the sodium becomes saturated and precipitates out the insoluble impurities. At 121°C (250°F), the solubility of oxide in sodium is about 5-10 ppm. Figure 2.3 displays a sectional view of the cold trap. Sodium exits the primary flow at downstream side of the pump cell and enters the cold trap. Here sodium is cooled to about 121°C (250°F) by air flowing across the outside finned surfaces of the cold trap. Any precipitated impurities will be trapped by the stainless steel wool. Purified sodium then flows out the top of the cold trap vessel and returns to the main stream at the inlet of the surge tank.

2.2.4 SURGE TANK: The surge tank functions as:

7

1. A gas disengagement chamber to remove any gas void in sodium stream.

2. Hot trapping device to remove oxygen from liquid sodium.

Hot trapping is termed as the addition of a highly reactive material, in solid form, into the liquid sodium system to chemically bind an impurity thus effectively isolating it from further reaction in the system. Hot trap can maintain an oxygen concentration lower than that attainable with cold traps. Zirconium has proved to be a useful getter for oxygen since its oxides, from thermodynamic point of view, are very stable. The theoretical equilibrium concentration of oxygen in sodium system hot trapped with Zirconium at 1200°F has been calculated to be less than 7×10^{-6} ppm.
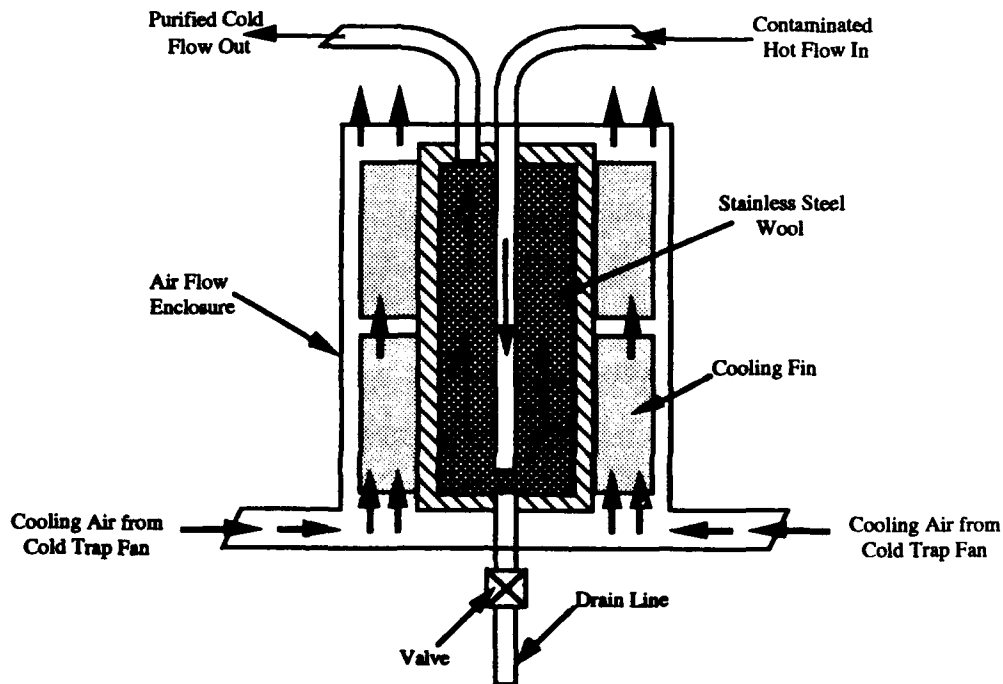
Figure 2.3: Cold Trap Sectional View

Surge tank inlet and outlet are at the bottom, separated by a stainless steel barrier. Two baffles, one is stainless steel and the other is Zirconium, are

8

suspended within the surge tank, one on each side of the barrier. The stainless steel baffle functions as a filtering device while the Zirconium baffle hot traps any oxygen in the sodium. The surge tank also had a spout through which sodium was changed into the system. Figure 2.4 shows the surge tank sectional view.
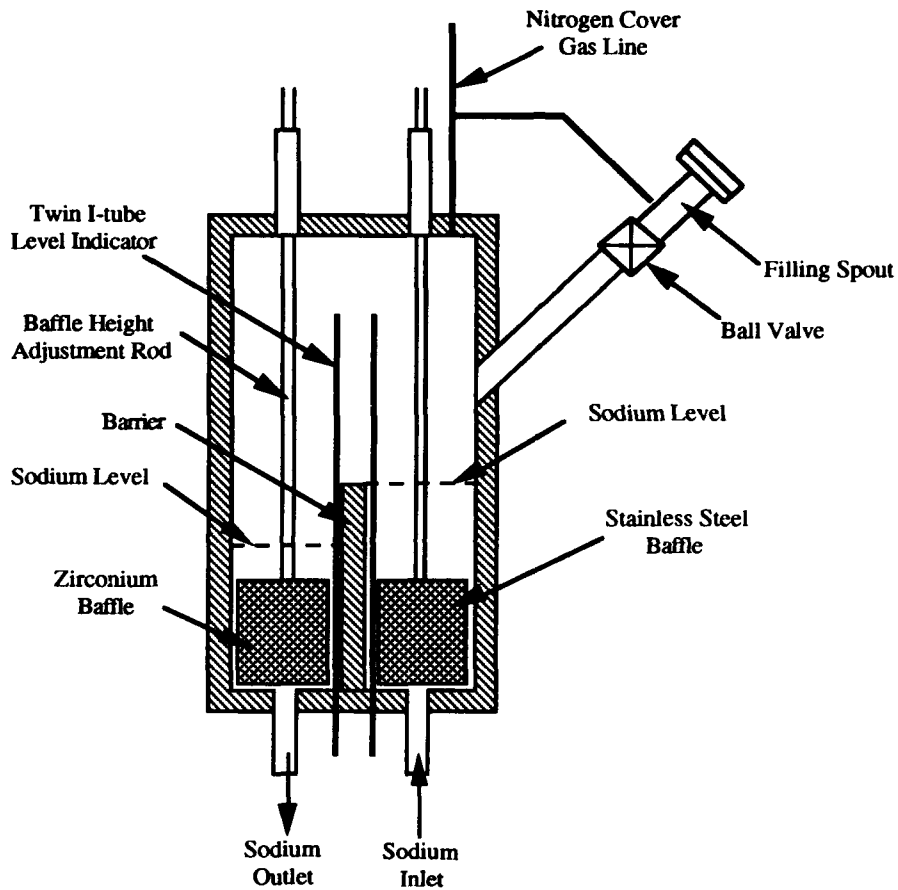
Figure 2.4: Sectional View of Surge Tank

2.2.5 ECONOMIZER: For safety purposes, it is preferred to keep the pump cell temperature between 315 and 425°C (600 and 800°F). The test cell,

however, is at 727°C (1340°F) in normal operation. To maintain such a large temperature difference, the economizer is used. The economizer allows heat to be transferred from the hot downward flow to the cool upward flow; thus eliminating any heavy heating or cooling of the sodium. The economizer consists of two concentric-tube counter flow heat exchangers. The hot sodium flows in the tube section while the cold sodium flows in the annulus section of the heat exchanger. Up to 300°C (572°F) temperature increase/decrease has been recorded across the economizer.

2.2.6 TEST CELL: It was desired to have a vessel in which sodium can flow across an inserted heat pipe to provide a realistic thermal loading. This vessel must be leak proof while allowing the heat pipe to be easily replaced. Because heat pipe wall was constructed of inconel, it is necessary to uses inconel compression fitting to lock the heat pipe in its place. Leaking problem arose when attempting to weld the inconel fitting to the stainless steel vessel. The final solution was to use an inconel female pipe threaded - compression fitting coupling to connect the heat pipe to the test cell. The difference in thermal expansion at the pipe threaded stainless steel - inconel fitting provided a necessary sealing at elevated temperature. Figure 2.5 illustrates the test cell with heat pipe installed.
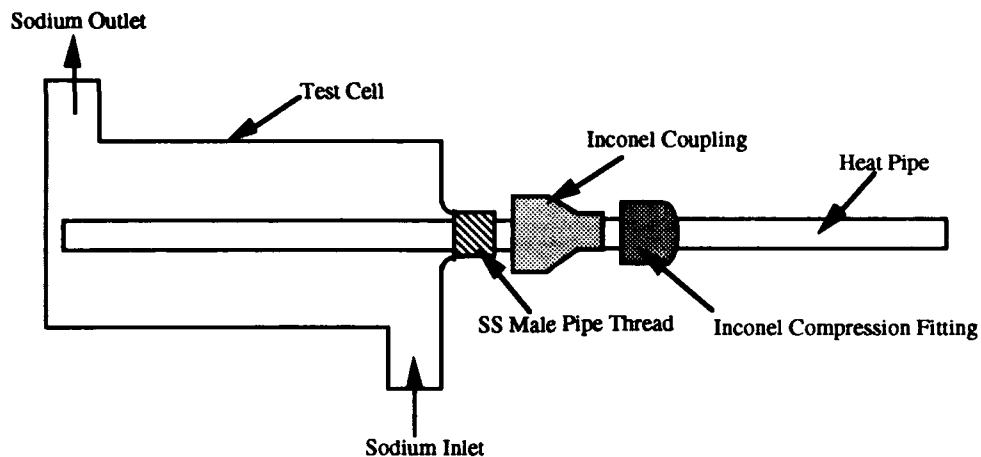
Figure 2.5: Test Cell with Heat Pipe Installed

2.2.7 ELECTROMAGNETIC PUMP: The sodium loop utilized a conduction electromagnetic pump to circulate the liquid sodium. The strongest advantage of electromagnetic pump was its high reliability since no parts are in contact with liquid sodium and no seals are required. The ability to service the pump without opening the piping system was another advantage. The major disadvantage was the loss of flow in the presence of any gas void in the liquid stream. In electromagnetic pump, liquid sodium is driven through the pump cell by the pressure gradient resulted from the interaction of electrical current and magnetic field which passed through the same space in liquid sodium simultaneously. This principle is illustrated in Figure 2.6. A current is conducted to liquid sodium, and from it, by the silver straps which were bonded to the left and right sides of the pump cell. At the same time, a magnetic field is produced on the top and bottom surfaces of the pump cell by the electromagnets. The current which passed through the sodium is typically thousands of amperes at a fraction of one volt. Figure 2.7 shows the pump cell with silver insert for maximum electrical conductivity.

11
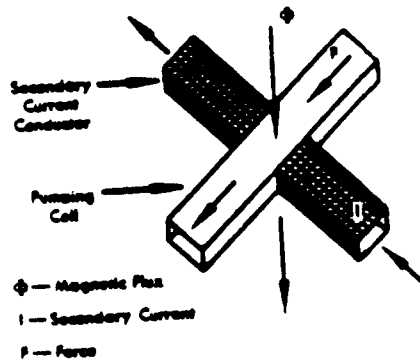
Figure 2.6: Operational Principle of Electromagnetic Pump
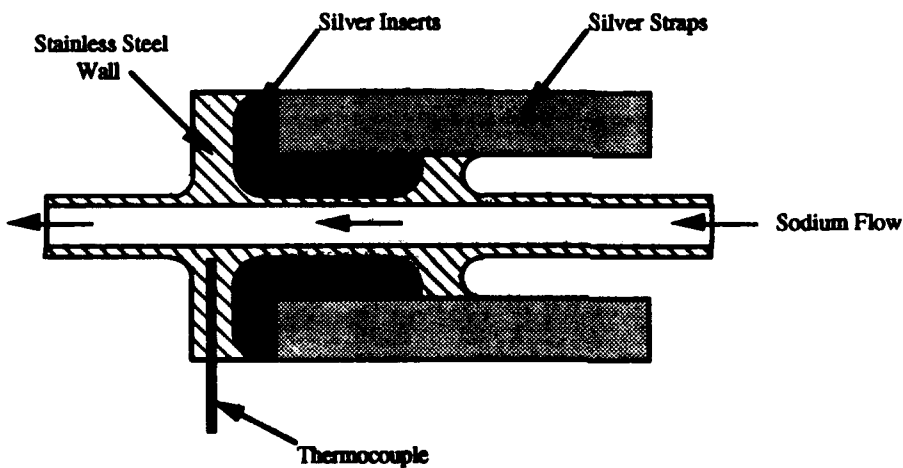
Figure 2.7: Pump Cell

2.2.8 ELECTROMAGNETIC FLOW METER: There are two E.M. flow meters used in the sodium loop; one located downstream from the pump cell prior to the bypass line, the other located at the exit of the test cell. An E.M. flow meter used in the sodium loop is shown in Figure 2.8. Electromagnetic flow meter operates on the principle that an electromotive force, emf, is generated in the conductor moving in a magnetic field. The emf is given by the relation:

$$E = B L V x 10^{-5}$$

where E is the emf (mV), B is the magnetic flux density (Gauss), V is the mean liquid velocity (cm/sec), and L is the length of the conductor (cm). Figure 2.9 illustrates the operational principle of the E.M. flow meter. The advantages of electromagnetic flow meter are extremely low pressure drop, no moving parts, and no penetration of the piping structure. The calibration of these flow meters, however, poses some difficulties due to the dependency of output voltage on liquid temperature, magnet temperature, and some other factors.

Mounting Plate

Permanent Magnet

+

Stainless Steel Pipe

Liquid Sodium

Copper Wire to Voltmeter

Stainless Steel Electrode

Figure 2.8: Electromagnetic Flow Meter

13
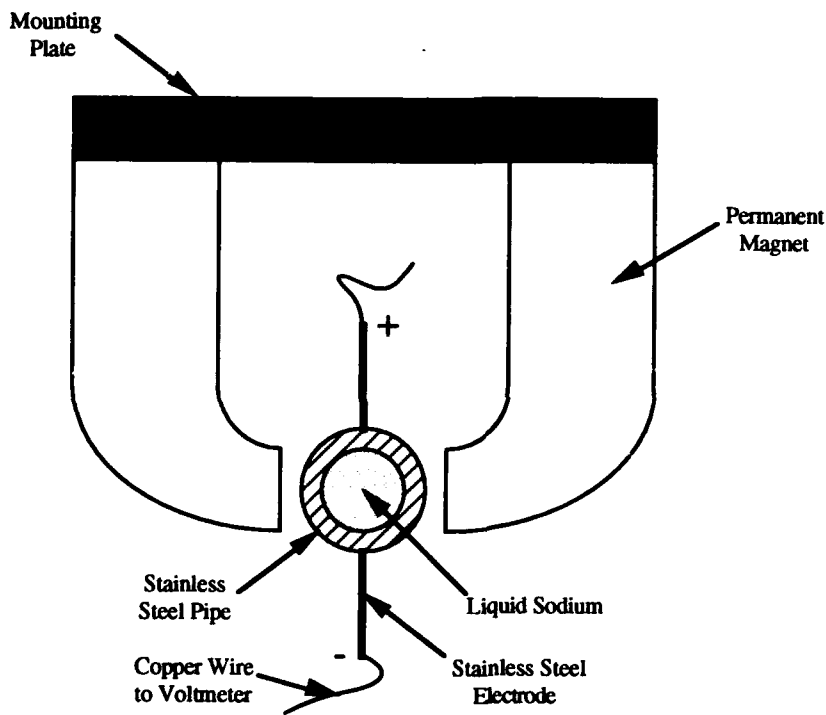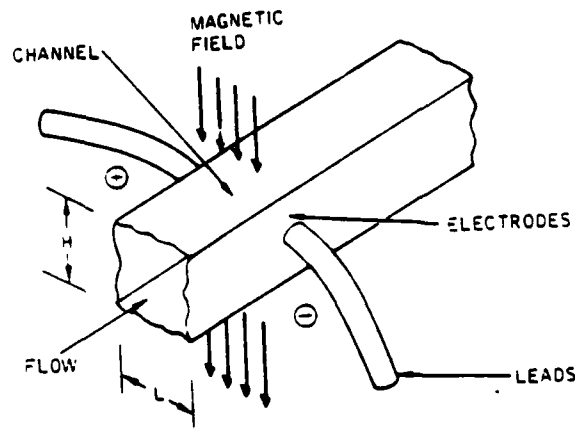
Figure 2.9: Operational Principle of E.M. Flow Meter

The output voltage, in principle, is exactly the above emf when measured with an infinite impedance voltmeter. In practical flow meter, however, there are several factors that affect the output voltage. The duct or pipe is an electrical conductor; hence, it constitutes an electrical shunt that results in a drop in the output voltage. This voltage drop is the function of pipe diameters and electrical resistivities of pipe and liquid sodium. The reduction factor is:

$$f = \frac{2D_i D_o}{D_o{}^2 + D_i{}^2 + (\rho_l/\rho_w)(D_o{}^2 - D_i{}^2)}$$

where D_i, D_o are inside and outside diameters of pipe; and ρ_l and ρ_w are

14

electrical resistivities of liquid sodium and pipe wall, respectively. Since the resistances are temperature dependent (sodium resistivity increases from 9.64 Ω-cm at 98°C to 29.8 Ω-cm at 500°C), the output voltage is also temperature dependent. In addition to the shunting effect of wall, liquid metal in the end regions (i.e., regions upstream and downstream from the central region comprising the electrodes in a uniform field) also constitutes a shunting effect.

Another factor which affects the output voltage is the magnetic field distortion. Liquid sodium entering or leaving the E.M. flow meter experiences the magnetic flux gradient. This generates an eddy current, in liquid metal, which in turn induces the magnetic field. Since the magnetic flux gradient is positive at the entrance of the flow meter and negative at the exit, the eddy-current-induced field at the entrance side is opposite that at the exit side. Superimposition of these fields upon the primary field results in a distortion of the field. This distortion generally shifts the maximum flux location downstream; thus, the electrodes may not give the highest output voltage. The amount of shift is the function of liquid velocity, conductivity, etc.

The temperature dependence and, to some extent, time dependence of the magnetic flux density produced by the permanent magnet also affect the voltage. Another factor is the thermal emf generated at the stainless steel electrode - copper wire junction. If the two junctions were at the same temperatures, the produced emfs are the same; thus, they cancel each other, leaving the output voltage unchanged. However, due to the extremely low output voltage (0.6 mV for a flow of 1 gal/min at 1000 K), a temperature difference of several degrees would definitely affect the output.

2.2.9 LEVEL INDICATORS: The sodium levels in surge tank and dump tank #1 are measured by twin one-tube level indicators installed inside each tank. A

15

schematic of one-tube level indicator is shown in Figure 2.10. Figure 2.11 presents an equivalent circuit for twin one-tube level indicator. If the input voltage is kept constant, the output voltage is directly proportional to the tube electrical resistance. The tube resistance is maximum when the tank is empty and drops to zero as the sodium level rises to the tip of the one-tube or higher. Thus, the output voltage is inversely proportional to the sodium level in tank. For the input voltage of 2 volts, the unamplified output signal when tanks are empty were measured to be 11.4 mV and 4.6 mV for surge tank and dump tank, respectively.

2.2.10 FILTER: Figure 2.12 shows a sectional view of the filter. It is located at the exit side of the surge tank.

2.2.11 COOLER: It is basically a squared-finned heat exchanger. The cooler lowers the sodium temperature before the sodium enters the pump cell. Since the cooler was located in the air intake duct, the amount of cooling can be controlled by adjusting the exhaust fan valve.

2.2.12 FROZEN SECTION: As the name implied, this section is normally frozen. It is used when extremely small sodium flow rate is desired at the test cell (below that attainable by lowering the pump voltage). The frozen section has proved to be useful in reducing the pressure, at the test cell, caused by thermal expansion of sodium during start up.
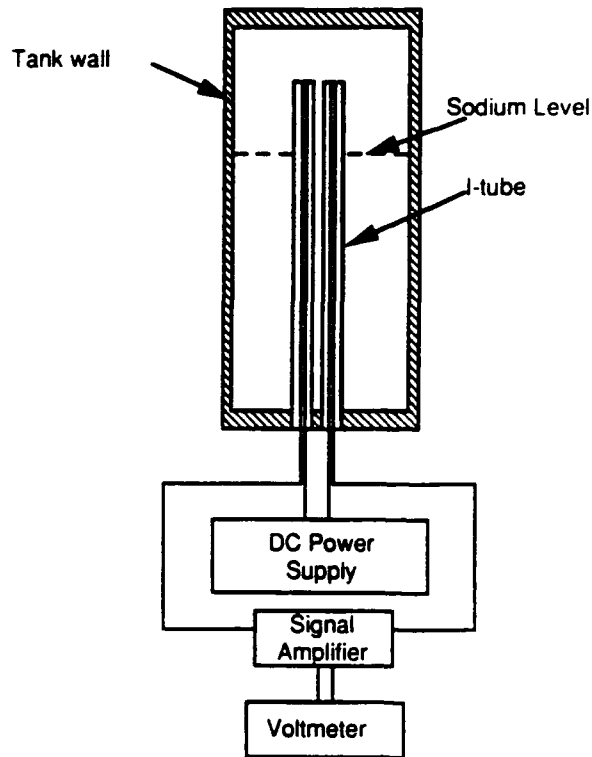
Figure 2.10: Twin *I-tube* Level Indicator
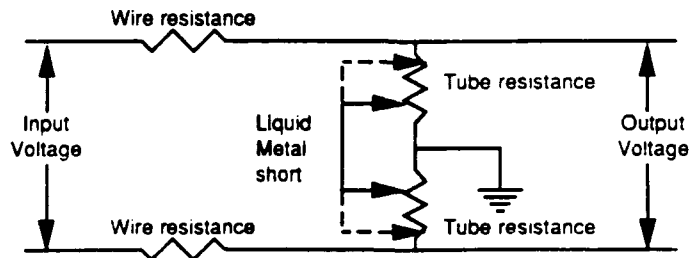
$$V_o = \frac{2 \text{ (Tube resistance)}}{2 \text{ (Wire resistance)}} V_i$$

Figure 2.11: Level Indicator Equivalent Circuit

17
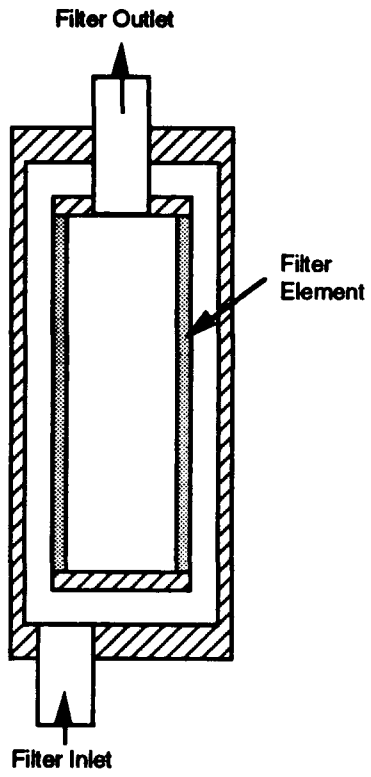
Figure 2.12: Filter Sectional View

2.3 SODIUM LOOP POWER INPUT AND CONTROL

The power input to the sodium loop was turned on or off by a relay whose coil power was controlled by two sensor/relays. These sensor/relays acted as a safety system and their descriptions can be found in the safety section of this report. Figure 2.13 illustrates the schematic of the electrical circuit of the sodium loop. The power to the electromagnetic pump was controlled by a variac thus allowing the sodium flow rate to be changed with ease.

2.3.1 SODIUM LOOP HEATER CIRCUIT

Thermal power input to the sodium loop was supplied by the tubular resistive heaters. These heaters were rated 41.7 watts per linear inch at 220 volts. They consist of a nichrome heating element, incolloy sheating and magnesium silicate insulation. The last 16 cm section of each end of the heater does not contain a heating element.

The heaters were installed lengthwise on the underside of most loop piping, except one section (test section 1) where the double heaters were installed with one on top and one on the bottom of loop piping. For the tanks, the heaters were bent in an accordion pattern and formed to the outer diameter of the appropriate vessel. Once the heaters were attached to loop piping/tanks by hose clamps, stainless steel shim stocks were tightly wrapped around to enhance the heat transfer between the heater and sodium. Both ends of heaters were bent outward and extended through the insulation for electrical connection. Because some heaters were longer than the available heating length of loop piping, the unused section of the heater was bent outward and attached with cooling fin to prevent heater failure from over-heating. The
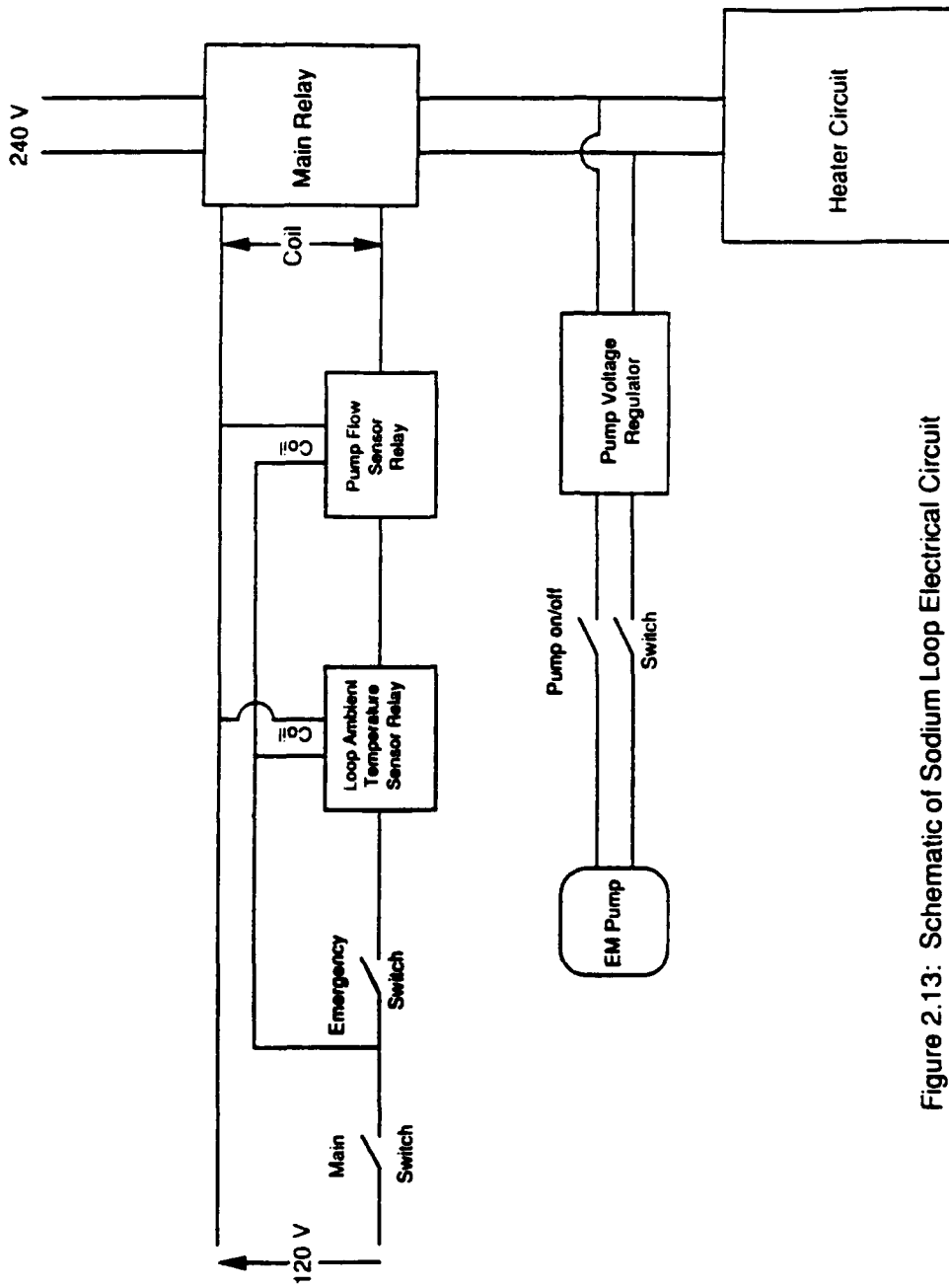
Figure 2.13: Schematic of Sodium Loop Electrical Circuit

electrical terminals of each heater were insulated with sock-type glass insulator to prevent any accidental short circuit.

Once the heaters and the stainless steel shim stock were in place, the insulation was added. The insulation material, used in loop, was known as cera-blanket with the thermal conductivity of approximately 0.15 W/mK and maximum service temperature of about 1450 K. Assuming the heat transfer coefficient of 10 W/m^{2}K, the insulation critical radius was calculated to be 1.5 cm (0.6 in). Thus the insulation thickness (equals the critical radius minus the pipe outer radius) must be at least 0.635 cm (0.25 in). Since insulation was purchased in 3.81 cm (1.5 in) thickness, it was decided to use double layers of insulation (7.62 cm or 3 in thick) on the test sections and tanks. The rest of the loop piping was insulated with single layer of insulation.

Figure 2.14 presents the heater circuit diagram. The heaters in sodium loop were grouped into nine heater circuits as summarized in Table 1. Except for test section 2, each individual circuit was regulated by a proportional gain controller. Each controller was responsive to a thermocouple. All heater-controller connections were made within the heater junction box. Figure 2.15 shows the wiring diagram within the junction box. The heaters in the parentheses were disconnected to reduce power consumption since they were not used in normal loop operation.

Figure 2.16 shows the locations and wattage of heaters on dump tanks, surge tank, cooler, cold trap and cold trap lines. Dump tank circuit was controlled by controller #1. As seen from Figure 2.16, there were five heaters in this circuit. Since the second dump tank was not used, heaters D4 and D5 were disconnected. Controllers #4 and #5 regulated power input to the cold trap and the cold trap lines, respectively. Actually, these heaters were used

21
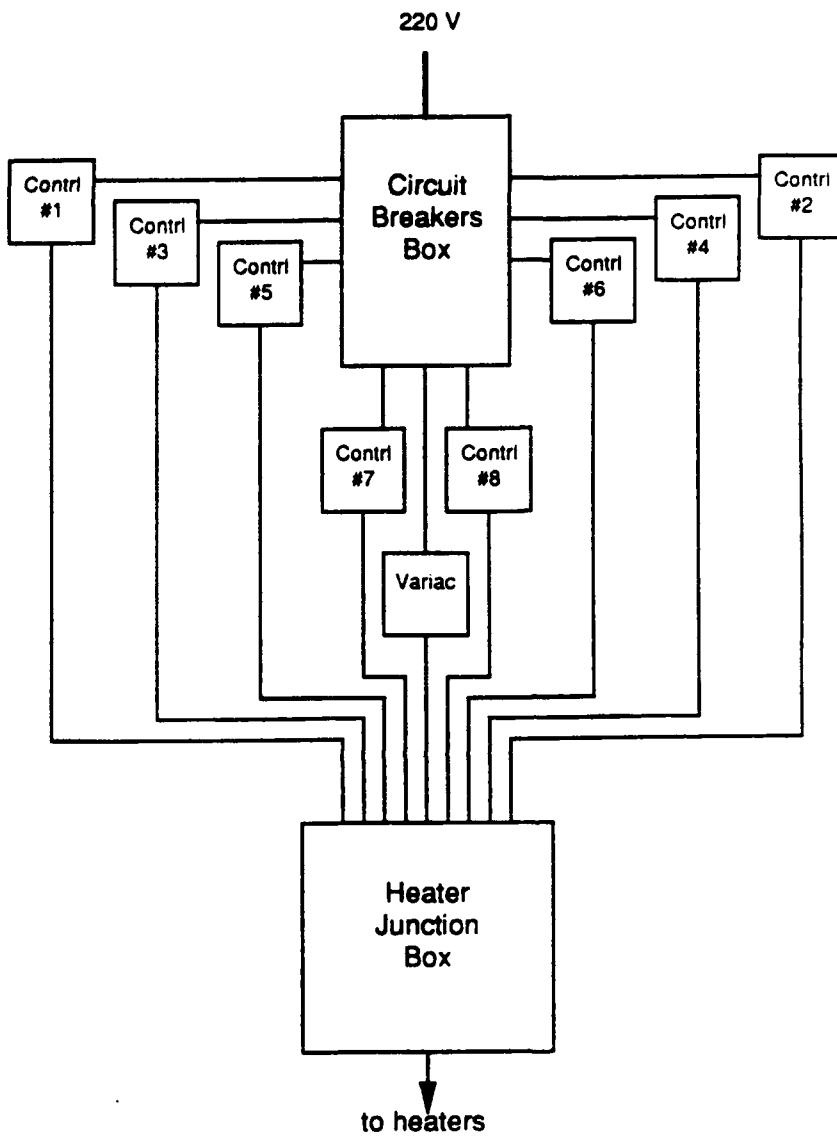
Figure 2.14: Heater circuit schematic

22
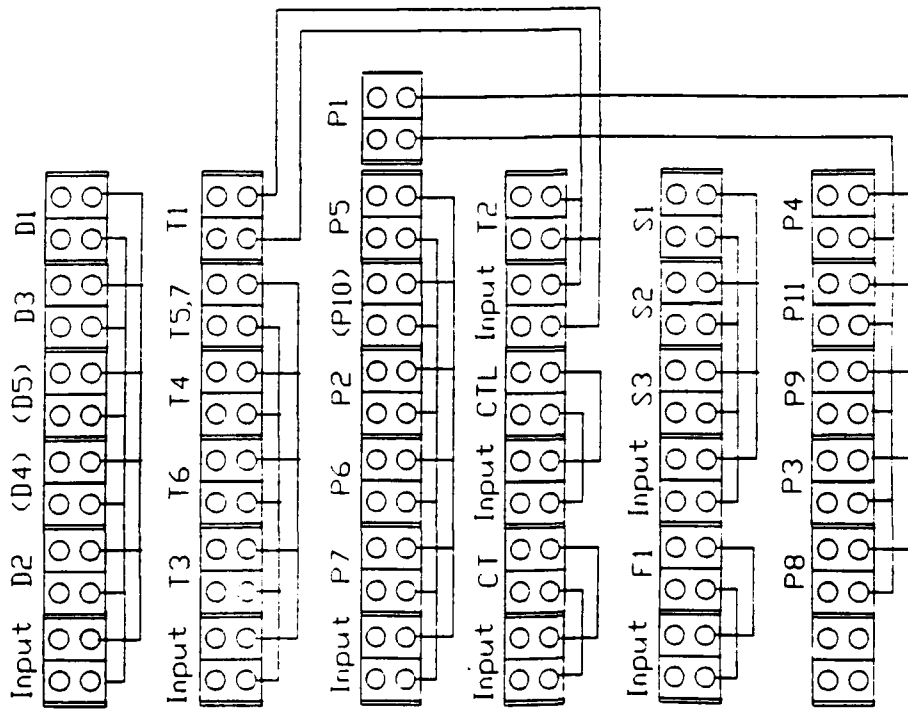
D1-5 --DUMP TANKS

T3-7 --TEST SECTION #1

T1-2 --TEST SECTION #2

P1-P11 --PROCESS

CT --COLD TRAP

CTL --COLD TRAP LINE

F --FROZEN SECTION

S --SURGE TANK

Figure 2.15: Wiring Diagram of Heater in Junction Box

23
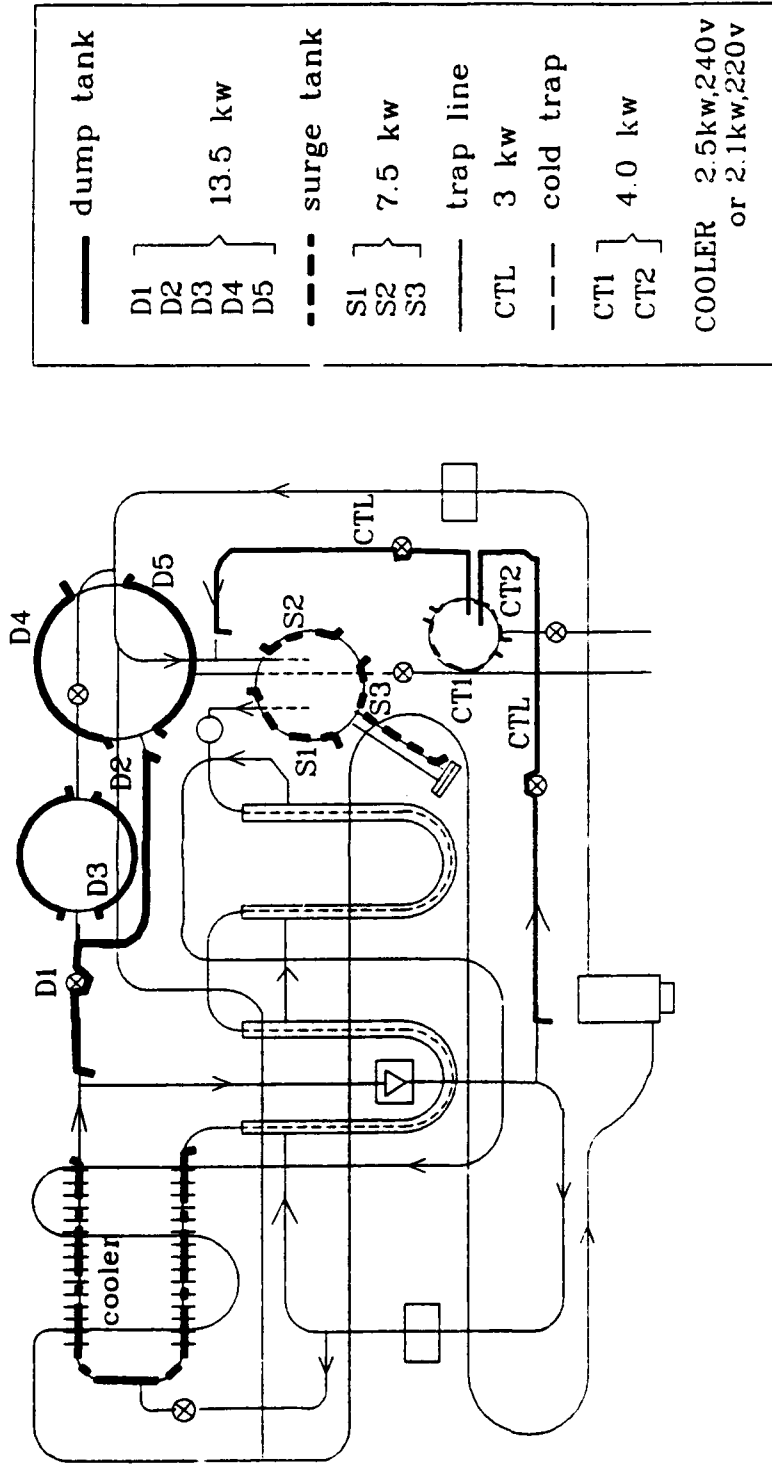
Figure 2.16: Location of Heaters on Dump Tanks, Surge Tank, Cold Trap, Cold Trap Line, and Cooler.

only to melt the sodium at the startup of the clean up cycle. Once flow is achieved in the cold trap, these heaters must be turned off to have the cooling effect on the sodium. Surge tank heaters were controlled by controller # 6. Heater S3, used to heat the filling spout of the surge tank during sodium charging, was disconnected for normal operation. Controller #7 regulated the power input to cooler heater. This heater was the same as those used in conventional ovens, thus safe to operate at full power in air. The cooler heater circuit was extremely important in regulating the pump cell temperature. When the loop is operating at low temperature, the cooler heater helped to maintain the pump cell temperature at a level that provides good flow characteristics.

TABLE 2.1: HEATER DISTRIBUTION

Heater Circuit	Wattage	Controlled by	Control TC
Dump tank	13.5 kW	Controller #1	TC# 20
Surge tank	7.5 kW	Controller #8	TC# 14
Cold trap	4 kW	Controller #4	TC# 26
Cold trap lines	3 kW	Controller #5	TC# 27
Test Section 2	3.2 kW	Variac	none
Test Section 1	9.8 kW	Controller #2	TC# 11
Frozen section	2.7 kW	Controller #6	TC# 30
Cooler	2.5 kW	Controller #7	TC# 31
Process & Economizer	13.8 kW	Controller #3	TC# 15

A diagram of heater location for process and economizer is presented in Figure 2.17. Controller #3 controlled this circuit. Heater #10 was
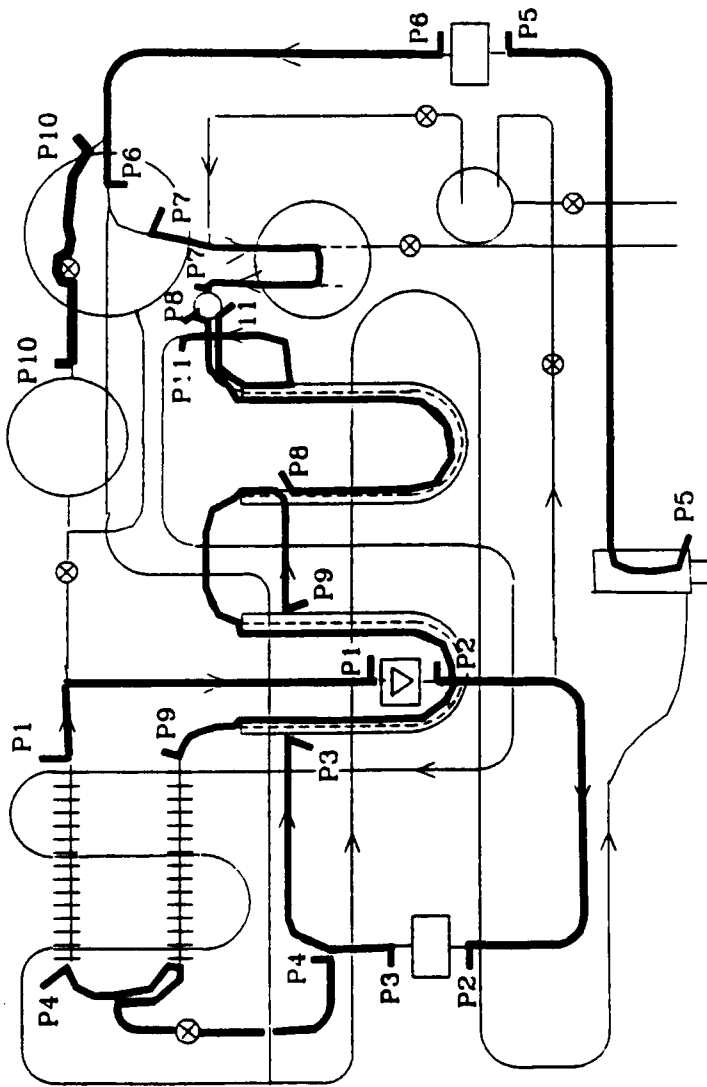
Process and Economizer

heaters	kw
P1–P1	1.3
P2–P2	0.8
P3–P3	0.8
P4–P4	1.3
P5–P5	1.8
P5–P6	1.3
P7–P7	1.3
P8–P8	0.8
P9–P9	1.8
P10–P10	1.3
P11–P11	1.3

Total power=13.8 kw

The 10 heaters are connected in parallel and controlled by a single controller.(#3)

Figure 2.17: Process and Economizer Heaters

disconnected for normal operation since that section was used only during sodium charging. A switch was installed for heater #5 which heated the test cell and the exiting line. This switch allowed the heater to be turned off during heat pipe testing.

Figure 2.18 illustrates the location of test section and frozen section heaters. The test section, which extended from the exit of economizer to the entrance of the test cell, was divided into two sub sections, namely test section 1 and test section 2. The test section 2 was between the exit of economizer and inlet of frozen section. The section between the inlet of frozen section and inlet of test cell is the test section 1. Such division allows the loop to operate without sodium entering the test cell. Since the test section 2 was used to calibrate sodium flow rate, its power inputs were controlled by a variac. Test section 1, where major heat is added to the loop, was installed with double heaters; thus increased the power input to 83.4 watt per linear inch at 220 V. The test section 1 heaters were controlled by controller #2. The frozen section heater received its power from controller #4. As the name implied, this section remains frozen during most normal operations.

2.3.2 TEMPERATURE MEASUREMENT AND CONTROL:

Sodium loop utilized 31 type-K thermocouples to monitor temperature within the loop. These thermocouples were attached to the outer surface of the loop piping or tank by hose clamps, and their outputs were assumed to be the true sodium temperature due to the extremely high heat transfer coefficient at the loop piping inner surface. The thermocouple circuit consisted of a multiple (24) jack-type thermocouple connectors, a thermocouple switch and a digital

Test Section

#1

T3–T3
T4–T4 } 5.4 kw
T5–T5

T6–T6
T7–T7 } 4.4 kw

#2

T1–[1]
T2–T2 } 3.2 kw

FROZEN
SECTION
2.7 KW
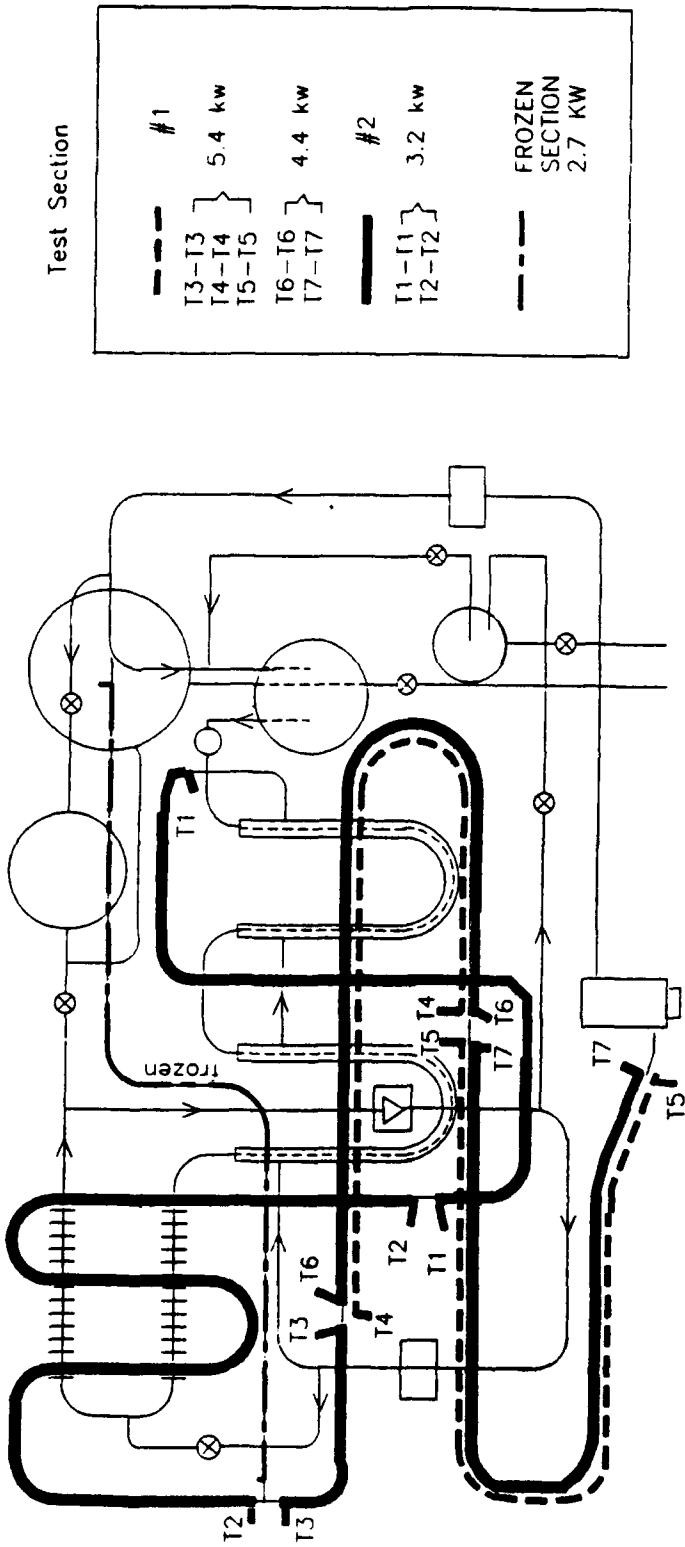
Figure 2.18: Heater Locations of Test Sections
and Frozen Section.

28

thermocouple thermometer. Eight controlling thermocouples were connected to connectors numbered 1 to 8 which were then connected to eight controllers; 15 thermocouples were connected to connectors numbered 9 to 23 which were then connected to the thermocouple switch. Eight other less important thermocouples were connected directly to the thermocouple switch. The outlet of the thermocouple switch was connected to connector #24 which was then connected to the digital thermometer. The above setup allowed quick replacement of controlling thermocouples and easy monitoring of loop temperature distribution. Figure 2.19 shows the locations of thermocouples throughout the sodium loop together with their designated positions on the connectors and thermocouple selector switch. The descriptions of thermocouples is given in Table 2.2. For safety purposes, the test section 1 heater and the pump cell thermocouples, TC# 23 and 29, respectively, were connected to separate thermometers for continuous monitoring of the temperatures.

Besides these thermocouples, there were other thermocouples used for flow rate calibration and determination of heat gain/loss at the test cell. The locations for these thermocouples will be explained in the calibration section and heat pipe testing procedure.

Figure 2.19: Locations and Wiring of Thermocouples

TABLE 2.2: THERMOCOUPLES

T/C #	Description	TC connector #	TC switch #
1	Pump cell outlet	11	11
2	Economizer cold inlet		2
3	Economizer		3
4	Economizer	18	18
5	Economizer cold outlet		5
6	Test Section 2	13	13
7	Test section 2	20	20
8	Test section 2 outlet	14	14
9	Test section 1	9	9
10	Test section 1	10	10
11*	Test cell inlet	2	
12	Test cell	12	12
13	Test cell outlet		6
14*	Surge tank	8	
15*	Economizer hot inlet	3	
16	Economizer hot outlet	16	16
17	Cooler at bypass	17	17
18	Cooler outlet		8
19	Pump cell inlet	19	19
20*	Dump tank #1 (tall)	1	
21	Dump tank #2 (short)	21	21
22	Dump tanks connecting line	22	22
23**	Test section 1 heater		
24	Dump tank drain line		24
25	Cold trap inlet line	23	23
26*	Cold trap	4	
27*	Cold trap outlet	5	
28	By pass line at valve	15	15
29**	Pump cell		
32*	Frozen section	6	
31*	Cooler	7	

* Control thermocouple
** Connected to separate thermometer for continuous monitoring.

3. SAFETY SYSTEM

Due to the unusually high reactivity of sodium, the liquid sodium loop must be equipped with a number of safety devices to prevent or to handle fire in case of any accidental leakage. These devices ranged from the simple passive sodium containment system to the active scrubber system.

3.1 SODIUM CONTAINMENT

It was decided that sodium would be stored in loop piping and surge tank. Dump tank will be used only during charging, dumping and emergency procedures. This is done to provide a larger surface area for heating and cooling, thus shorten the time period during which sodium is at high temperature. On the average, it took about 11/2 hours to bring the system from room temperature to the operation temperature of 1000K, and 21/2 hours to cool the system from 1000K to sodium freezing temperature (98°C); comparing to 4 hours heat up time and 8 hours cool down time if leaving sodium in the dump tank.

Exposing sodium to larger surface area, however, increases the chance of sodium leakage. To assure that leakage does not happen, all joints in the loop were sleeve welded. Sleeve weld also has advantage over butt weld: in butt welding of pipe, the welding material usually penetrates the welding surface into flow area thus restricting the flow; whereas in sleeve welding, the flow area remained unchanged. Figures 3.1 and 3.2 illustrate the typical butt and sleeve weld, respectively.

Another means of sodium containment was the stainless-steel shim stocks which were tightly wrapped around the pipe and heater. Insulation layer

and aluminum tape around the loop piping are additional barriers to any leakage from exposure to air. It has been noted that sodium, contained within the insulation material, reacted slowly at high temperature yielding a greenish-colored product that visually does not react with air or water. Thus a relatively small leakage of liquid sodium could be neutralized by containment within the insulation material. Figure 3.3 showed a cross section of the loop piping with shim stock, insulation and aluminum tape as leakage containment.
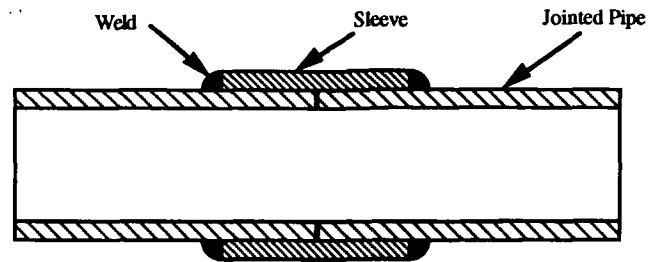

Figure 3.1: A Typical Sleeve Weld.
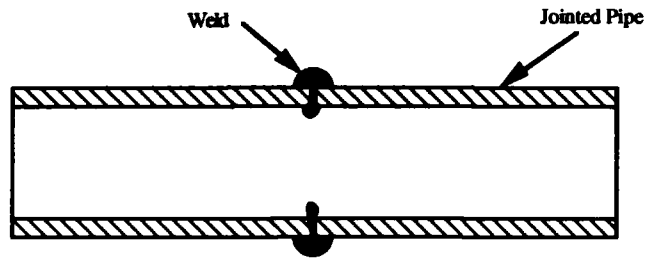
Figure 3.2: A Typical Butt Weld.
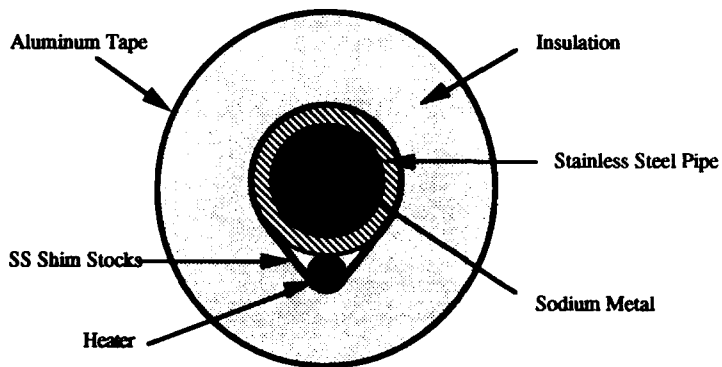
Figure 3.3: Sodium Containment.

In addition to the above containment system, steel balls were placed in the pan below the loop piping. These steel balls act as a heat sink for rapid cooling and/or solidifying any liquid sodium that leaked from the system.

3.2 LEAKAGE PREVENTION AND DETECTION

The sodium loop design maximum temperature was 950°C at 10 psig. For the single layer insulation line, the 150V power input could raise the temperature to about 920°C without sodium flow; while as in double layer insulation - double heater line, this temperature can be even higher (980-1000°C). Also the electromagnetic pump acts as heater if there is no flow. Thus, if a sudden loss in sodium flow went undetected, the result would be catastrophic.

A sensor was installed to solve this problem. This sensor measures the voltage output from the E.M. flow meter. When the output voltage dropped below a certain preset value, the sensor activates an internal relay to shut down the whole loop. As the loop was shut down, the sensor must be reset to restart the loop. This prevents the accidental start-up prior to the total inspection of the loop.

A similar device was installed in an attempt to detect any leakage or fire in the loop. Five thermocouples, located at different locations in the loop vault, were connected parallelly to a temperature sensor. Together, they output an average ambient temperature in the loop. The thermocouple locations are as follows: 1) Directly below the fitting of test cell; 2) Directly below pump cell; 3) Below dump tank valve; 4) Below economizer and surge tank; and 5) Near exhaust air exit. At these locations, sodium is most likely to leak, or fire is most likely to be detected. The sensor was normally set to turn off the loop electrical power at temperatures higher than 80°C (with test cell temperature at 730°C and cooling air vent partially opened, loop ambient temperature was about 70°C). If any of these thermocouples registered an unusually high temperature

35

presumably from hot liquid sodium or fires, the average temperature would increase above the preset value. This would trigger the internal relay to shut down the loop.

3.3 EMERGENCY COOLING:

In an event of leakage, it is preferred to handle sodium in solid form rather than in liquid form. Moreover, liquid sodium at relatively low temperature poses less a threat than at high temperature. Consequently, a liquid carbon dioxide system was installed. Since carbon dioxide fire extinguisher has little effect on sodium fire, the purpose of this system is to cool and/or solidify sodium liquid and vapor. Upon activation of the toggle switch, a solenoid valve will open and discharge liquid CO_2 to various locations in the loop for cooling purposes.

Another cooling technique utilizes the use of compressed air flowing through a series of flattened copper tubes placed underneath the dump tank. During emergency (leakage) situation, the dump tank valve is opened allowing liquid sodium to flow, by gravity, into the dump tank. There, heat is gradually removed by the compressed air flowing underneath the dump tank.

3.4 GAS PRESSURE RELIEF:

In normal operation, the cover gas pressure was set at 5-8 psi. Decreasing this pressure could significantly reduce amount of leakage if one does occur. The cover gas system has two pressure relief valves, one for the surge tank and other for dump tank. Normally, the gas pressures in dump and surge tanks were kept the same (pressure equalizing valve was opened). Thus, only one regulator and one relief valve were needed to control the

system gas pressure. Because the cover gas system was located inside the loop enclosure, an extension arm was installed to surge-tank-side relief valve to allow access from the outside. This eliminated the immediate hazard of opening the loop enclosure during leaking or fire situations.

3.5 SCRUBBER SYSTEM:

Sodium fires produce toxic smoke which must be removed from the laboratory and neutralized before releasing to the atmosphere. A 3650 cmfs blower moved air from the exterior of the building into the loop enclosure. Inside the enclosure, the air stream passed across a finned heat exchanger providing a neccessary cooling before exit through the exhaust pipe which led to the scrubber system. The air flow rate is regulated by a sliding vent valve located at the exhaust exit. Figure 3.4 shows the loop enclosure air flow.

The contaminated air enters the scrubber where it comes in contact with water being sprayed from the top of the scrubber thus providing the neccessary neutralization. Leaving the scrubber, the air carries with it large amounts of water vapor which were removed at the separator. Clean air is then released to the atmosphere. The schematic of air and water flow of the scrubber system is shown in Figure 3.5.

The pH level in primary scrubber water was monitored by a pH sensor installed at the pump inlet. The output of this sensor was fed to a programmable pH controller which was mounted on the control cabinet of the liquid sodium loop. In the event of a sodium fire, the water reacted with sodium vapor inside the primary scrubber and became extremely basic. When the pH level of the water exceeded a preset value, the pH controller will activate a chemical pump which pumps a proportional amount of dilute hydrochloric acid (HCl) into the

primary storage tank.
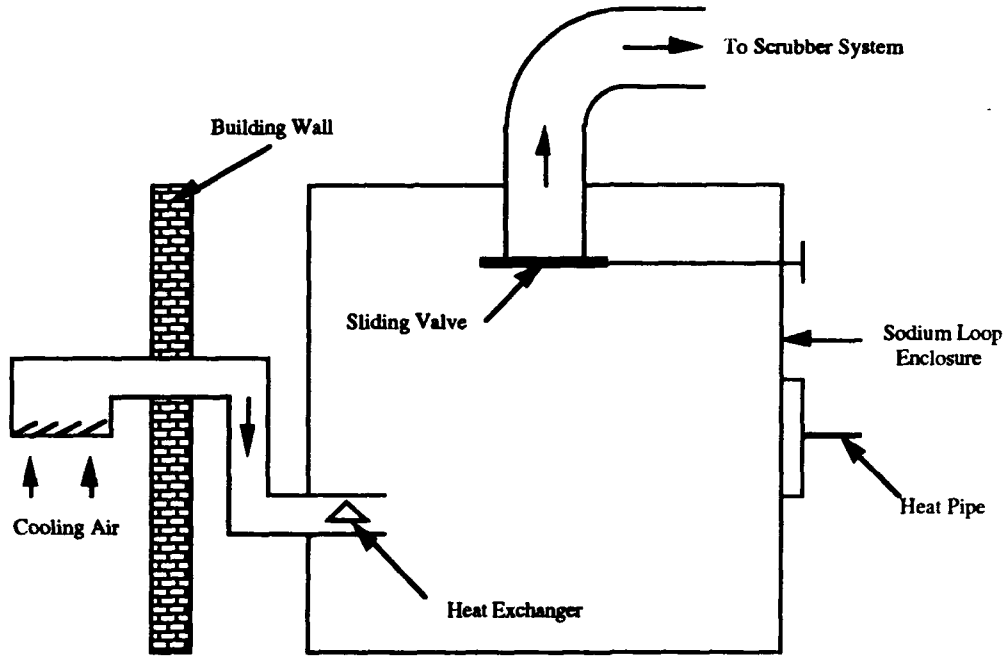
Figure 3.4: Loop Enclosure Air Flow

There is an auxiliary scrubber system to be activated in case of primary system failure. It is assumed that the posibility of primary blower failure is very small; thus, there are only two cases in which the primary scrubber system failed: power outage and pump failure. Since power outage stops the pump, installing a pressure switch at pump exit will detect both cases. When the pump exit pressure drops below 40 psig, the pressure switch closes allowing the auxiliary system to be powered by a battery-backup 120V power supply. A toggle switch installed in series with the pressure switch allows the auxiliay
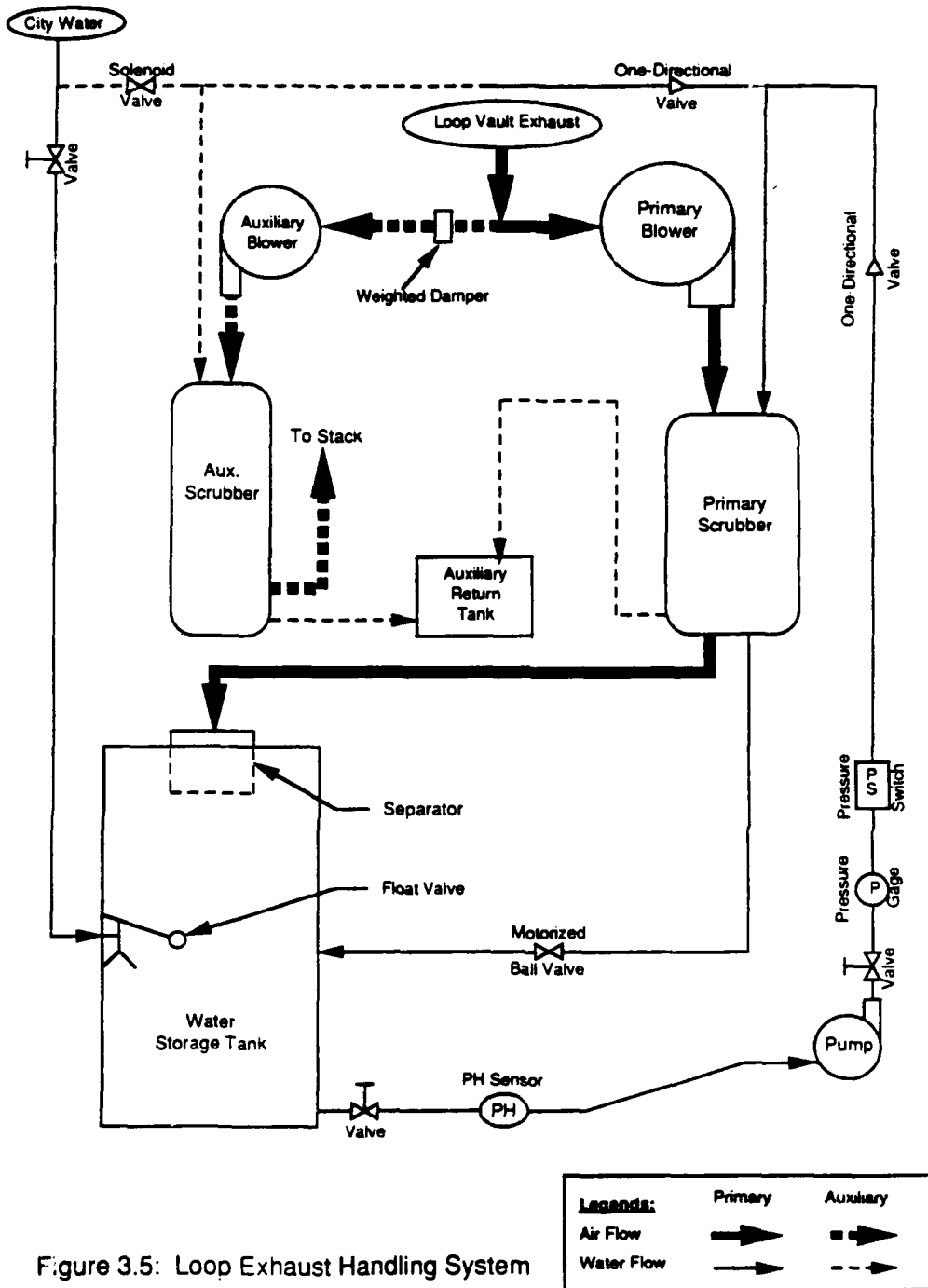
Figure 3.5: Loop Exhaust Handling System

The figure contains the following labels:

City Water

Solenoid Valve

One-Directional Valve

Valve

Loop Vault Exhaust

Auxiliary Blower

Primary Blower

Weighted Damper

One-Directional Valve

To Stack

Aux. Scrubber

Primary Scrubber

Auxiliary Return Tank

Separator

Float Valve

Water Storage Tank

Motorized Ball Valve

Pressure Switch P S

Pressure Gage P

Valve

PH Sensor PH

Valve

Pump

Legends:
Air Flow — Primary / Auxiliary
Water Flow — Primary / Auxiliary

system to be turned off manually. Figure 3.6 shows the electrical circuit of the auxiliary scrubber system. Upon activation, the auxiliary blower is turned on; solenoid valve is opened allowing city water to replace the pump; the ball valve is closed. City water is sprayed into both scrubbers. In the auxiliary unit, water exits to auxiliary storage tank. In the primary scrubber, because the ball valve is closed, water level rises to higher level, where it cuts off the air flow, then exits through a high-rise spout into storage tank. This design was to assure that the auxiliary blower removes air from the sodium loop but not from the primary scrubber. Figure 3.7 illustrates the water level in the primary scrubber during auxiliary cycle.
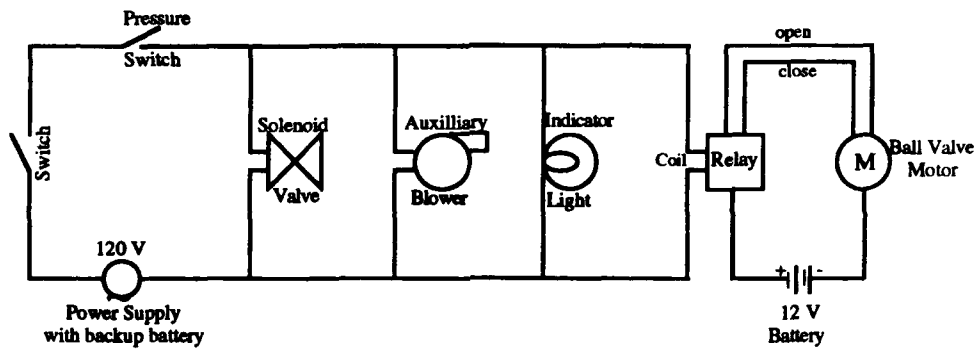
Figure 3.6: Electrical Circuit of the Auxiliary Scrubber System.
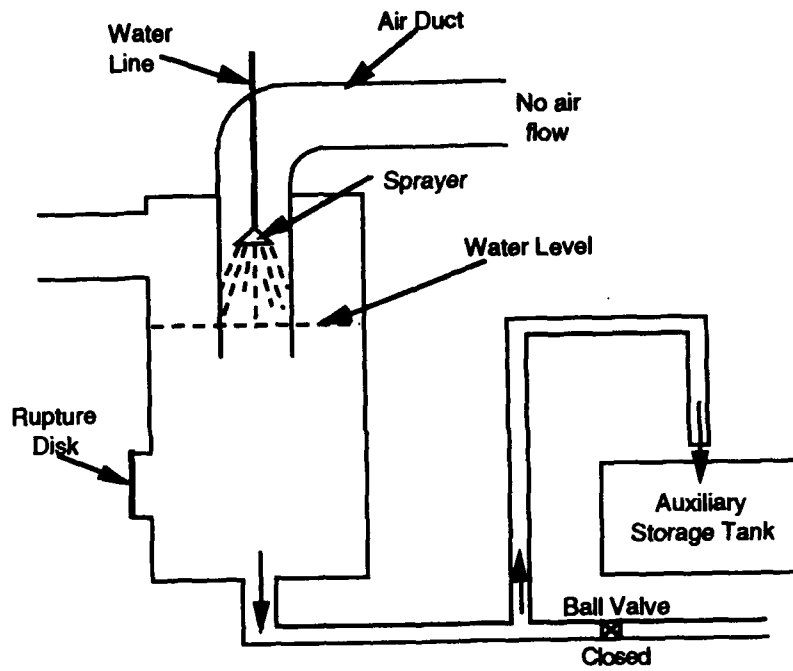
Figure 3.7: Water Level in Primary Scrubber during Auxiliary Cycle

4. SODIUM LOOP IMPROVEMENTS

The following are the summaries of the changes or improvements to the sodium loop:

1. All joints were sleeve welded.

2. All loop piping were of same size (0.840x0.109 stainless steel 304).

3. Installation of loop ambient temperature sensor-interlock.

4. Installation of sodium pump flow sensor-interlock.

5. Installation of (remote) cover gas pressure relief valve.

6. Installation of air flow valve to regulate the cooling capacity of the cooler.

7. Fabrication of the new pump cell.

8. Installation of pump cover to prevent foreign objects and debris from interfering with pump operation.

9. Less insulation on loop piping and vessel for lower pump cell temperature and for quick cool down.

10. Modified emergency scrubber system to improve reliability.

11. Less sodium used (73% reduction).

12. Installation of drain line for dump tank #2.

13. New test cell and test section.

14. Installation of test cell heater switch to be turned off during heat pipe testing.

15. Installation of voltmeter for test sections and process/economizer.

16. Installation of cold trap cooling fan.

5. HEAT PIPE EXPERIMENT

5.1 EXPERIMENTAL DESCRIPTIONS

The physical dimensions and properties of the heat pipe used in this experiment are listed in Table 5.1. The evaporator section, 0.140 m (5.5") long, of the heat pipe was inserted in a test cell where it contacted with flowing liquid sodium entering the test cell at a temperature of about 1000 K and a flow rate of 0.0502 kg/sec (1.01 gal/min). A 0.267 m (10.5") condenser section was exposed to room air. The middle section, between the condenser and evaporator, was used to hold the heat pipe in place. A cylindrical shell radiant heater was used to provide the pulse heat load at the condenser section of the heat pipe. This heater was mounted on a sliding bench to provide an instant application of heat load to the heat pipe. Figure 5.1 presents the experimental set-up. Eight K-type radiation-shielded thermocouples were mounted on the outer surface of the condenser section of the heat pipe.

Table 5.1: Heat Pipe Dimensions and Properties

Total Length, m	0.457
Outer Diameter, m	0.0127
Inner Diameter, m	0.0103
Vapor core area, $\times 10^{-5}$ m^2	7.216
Vapor core radius, $\times 10^{-5}$ m	5.131
Shell and wick mass, g	208.0
Sodium mass, g	8.0
Shell and wick material	Inconel 617
Wick type	screen
Screen type	100x100 mesh
Wick permeability, $\times 10^{-10}$ m^2	4.2
Wick capillary radius, $\times 10^{-4}$ m	1.0
Wick cross-sectional area, $\times 10^{-5}$ m^2	3.71

Their locations are as follow:

- 2.54 cm (1") from the condenser end of the heat pipe, four thermocouples were installed, 90° apart from each other. These thermocouples measured the circumferential temperature distribution.

- four thermocouples were mounted on top of the heat pipe at the locations measured 7.62, 12.70, 17.78, and 22.86 cm (3, 5, 7 and 9 inches) from the condenser end of the heat pipe. These thermocouples, together with the top thermocouple from the circumferential group, determined the axial temperature distribution.
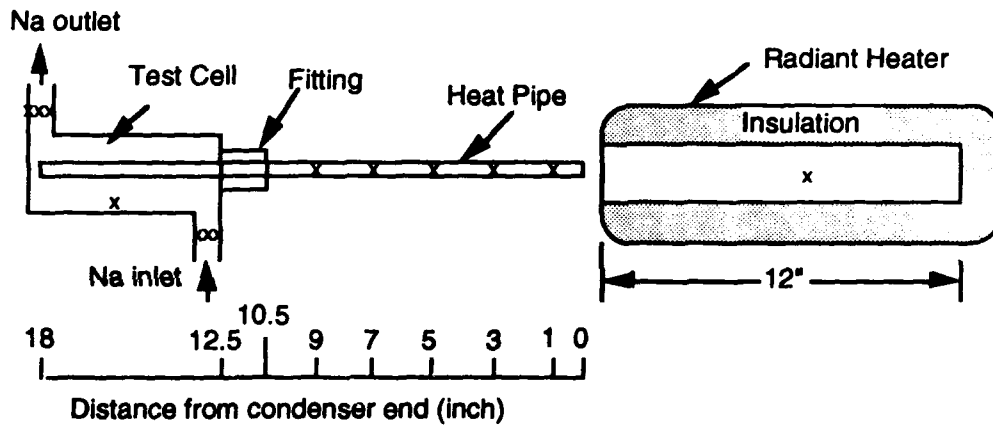
x   Thermocouple Locations

Figure 5.1:   Experimental setup

There were six thermocouples used in monitoring the sodium temperature at the inlet and outlet of the test cell, three on the inlet and three on the outlet. These thermocouples were clamped onto the outside surface of the loop piping. The measured temperatures were considered to be the sodium temperature due to the extremely high convective heat transfer coefficient at the inner surface of the loop piping (on the order of 10^4 W/m^{2}K). There were no direct means of

measuring the surface temperature of the evaporator section. A PC based data acquisition system was used to scan these thermocouples every 0.5 second.

5.1.1 CONDENSER HEAT INPUT DETERMINATION: As mentioned earlier, the condenser heat input was achieved with a cylindrical shell radiant heater. The electrical power input to the heater was controlled by a rheostat and measured with a voltmeter and an ammeter. This power, however, was not equal to the amount of heat transferred into the heat pipe due to the radiation and convection losses. Also if the heater were not operating at steady-state, there is additional loss of heat due to the change in thermal mass of the heater. To maintain the steady-state condition, a device shown in Figure 5.2 was constructed. It has the same external dimension and property as that of the heat pipe. This device, called heat pipe simulator, was inserted concentrically into the heater. With the rheostat on full power, the air flow was adjusted so that the device outer surface temperature was about that of the condenser section of the heat pipe operating in room air (685°C). The system was allowed to reach steady-state. The power input and heater surface temperature were recorded (heater surface temperature was about 1000°C). The simulator was then removed from the heater and the rheostat power was adjusted so that the surface temperature of the heater remained unchanged. This new power is the total heat loss from the heater at 1000°C. The net heat output by the heater operating at steady-state at 1000°C surface temperature was calculated to be 690 W.
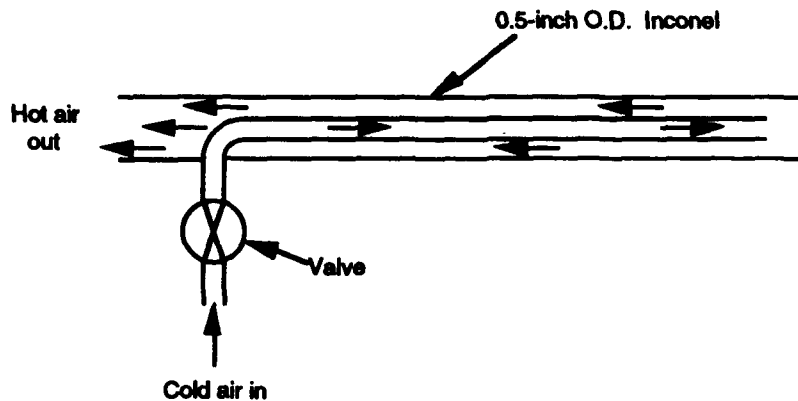
Figure 5.2: Heat Pipe Simulator

For all of the experimental runs, the liquid sodium at the test cell inlet was kept relatively constant at 730°C. The radiant heater, operating at full power with the heat pipe simulator inside, was kept in steady-state condition with the surface temperature of 1000°C. Once the heat pipe reached steady-state operation in room air, the heater was slid concentrically onto the condenser section (the simulator must be removed first!) The heater was left on for 60 seconds. The 60-second time interval was chosen as a compromise between maintaining steady-state condition of the heater and achieving steady-state operation of the heat pipe. The heater was then removed exposing the heat pipe section to room air.

Another set of experiments was conducted to study the heat pipe start up characteristics and their maximum heat transport limit. The heat pipe was allowed to operate at steady-state in room air. Then the condenser end was rapidly cooled by compressed air flowing axially at high velocity over its outer surface. The cooling air was maintained until the condenser was frozen. Once the condenser was frozen, the cooling air was removed and the heat pipe was

allowed to start up.

5.2 EXPERIMENTAL ANALYSIS

One objective of this research was the overall performance of the coupled sodium loop/heat pipe radiator when subjected to an adverse thermal loading condition. This overall performance can be represented by the amount of heat transferred to (or from) the sodium loop by heat pipe.The amount of heat delivered by the heat pipe can be determined by an energy balance of the test cell at steady-state (Figure 5.3):

$$q_{HP} = m\,C_p\,(T_o - T_i) + q_{loss} + q_{store} \tag{1}$$

where T_o and T_i are sodium outlet and inlet temperatures, respectively; m is sodium mass flow rate; C_p is the sodium specific heat; q_{HP} is heat delivered by heat pipe to (or from) the test cell; q_{loss} is the heat loss from test cell; and q_{store} is the rate of energy stored.
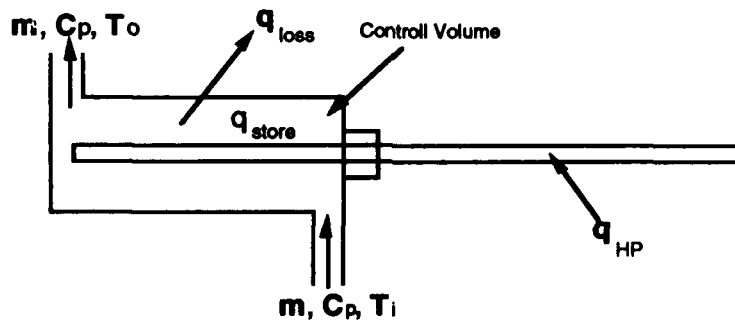

Figure 5.3: Energy Balance of Test Cell

In Eq. (1), the sodium mass flow rate and the total heat loss from the test cell

47

must be determined. The total heat loss from the test cell was found by insulating the condenser section of heat pipe ($q_{HP} = 0$); thus at steady-state, equation (1) became:

$$q_{loss}= m\, C_p\, (T_o - T_i)_{ss}, \text{ insulated heat pipe} \quad (2)$$

The test cell heat loss was considered to remain constant for all experimental runs. Figure 5.4 illustrates the calibration of the mass flow rate (see Appendix A for procedures). A best fit line drawn through the data points yields the slope or flow rate of 50.2 grams/sec.
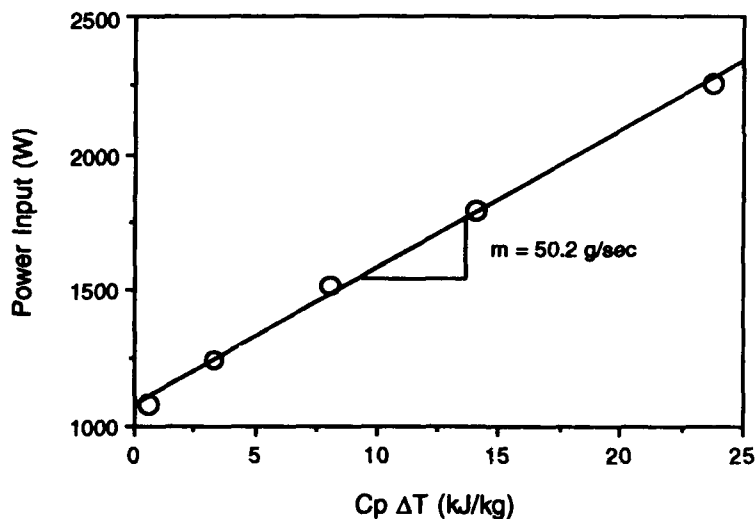

Figure 5.4: Flow rate calibration

The storage term in Eq. (1) is the rate of energy stored by the test cell and the sodium contained in it, and can be calculated using Eq. (3) with m and C being the mass and the specific heat, respectively.

$$q_{store} = (m_{cell}C_{cell} + m_{Na}C_{Na}) \, dT/dt \qquad (3)$$

The term dT/dt can be found from the experimental data with T being the average of the inlet and outlet temperatures of test cell.

Since the all of the data taken during the experiment are transient temperature data, it is necessary to determine the transient response of the thermocouples used in the experiment: three different sizes of thermocouple were used: 0.0625 inch, 0.020 inch, and 0.010 inch in diameter. Thermocouples measuring the circular distribution (located at 1inch from condenser end) were 0.0625 inch in diameter. Thermocouples monitoring the test cell inlet/outlet temperatures and 9 inch axial temperature were 0.020 inch in diameter. The remaining thermocouples (3, 5, and 7 inch axial) were 0.010 inch in diameter. The time response of thermocouple to a step change in temperature of a convective environment is:

$$\frac{T - T_\infty}{T_0 - T_\infty} = e^{-t/\tau} \qquad (4)$$

where T_0 is the thermocouple temperature at time zero, T_∞ is the true ambient temperature, T is the thermocouple temperature at any time t, and τ is the time constant for the system which is inversely proportional to the heat transfer coefficient. Three thermocouples (one from each size) were heated in the heater to 795°C; they were then moved into room air at 24°C. The plot shown in Figure 5.5 yields the time constants of 2.86, 5.65 and 18.35 seconds for 0.010 inch, 0.020 inch, and 0.0625 inch thermocouples, respectively. Since the time constant is inversely proportional to the heat transfer coefficient, the time

49

constant for the experiment would be smaller because conduction dominated the heat transfer process between the heat pipe and the thermocouples.
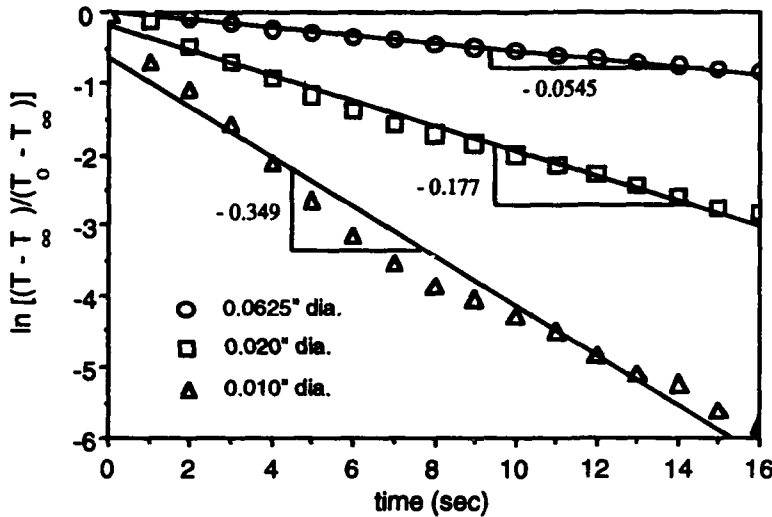
Figure 5.5: Time Response of Thermocouples to a Step Change in Ambient Temperature in Free Convective Medium

The theoretical heat transport limits of heat pipe used in the experiment were also calculated and graphically summarized in Figure 5.6.

5.3 EXPERIMENTAL RESULTS

Several thermal loading conditions at the condenser were studied and their descriptions are explained below.

1. Insulation to room air: The initially insulated condenser section was suddenly exposed to room air by removing the insulation.

2. Room air to full heater: After the heat pipe has reached steady state from loading condition 1, the heater was slid onto the entire condenser section.

50

Figure 5.6: Heat Transport Limit of Heat Pipe
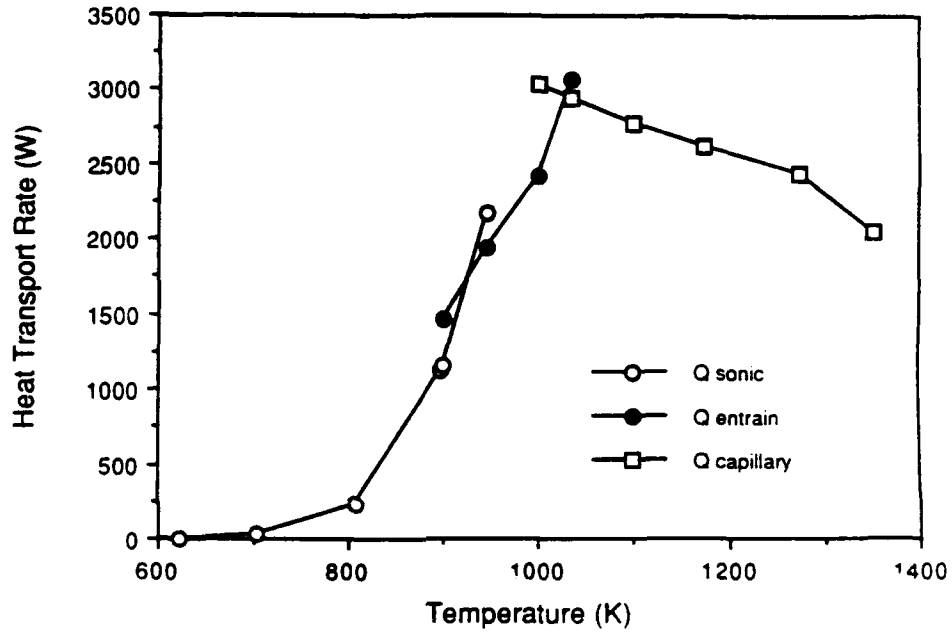
3. Full heater to room air: This condition was the reverse of condition 2. The heater was removed, re-exposing the condenser section to room air.

4. Room air to 1/2 heater: This condition was similar to the condition 2; however, only half of the condenser section was heated. The unheated half was next to the test cell.

5. Room air to 1/2 insulation and 1/2 heater: In this loading condition, the heat pipe was allowed to operate in room air when suddenly half of the condenser section was insulated while the other half was heated. The insulated section was between the heated section and the test cell.

The results of the experiment are presented in Figures 5.7a to 5.13. They are the plots of heat transferred by heat pipe to/from the sodium loop test cell (calculated from Eq. 1), the axially wall temperature distribution and circumferential temperature distribution as a function of time. The heat transfer data shown are the average quantities over the selected time intervals. The surface temperature at 7 inches was not shown due to thermocouple failure during the experiment.

Figures 5.7a,5.7b and 5.7c show the results of loading condition 1. When the insulation was removed, the heat pipe started immediately as seen in Figure 5.7a. From Figure 5.7a, the heat pipe, for a given test condition, removed heat at the rate of approximately 600 W at the end of the 60-second test run. The cooling mechanism at the condenser section is most likely to dictate this amount (the theoretical limit of the heat pipe as seen from Figure 5.6 was 4 times higher). It is important to note that the surface temperatures measured along and around the condenser section of the heat pipe were all the same at the beginning of this test. However, when the insulation was removed, large temperature variations were recorded as seen in Figures 5.7b and 5.7c. It is believed that the boundary layer induced by natural convection may have

52

Figure 5.7a: Heat pipe transient response

insulation to room air
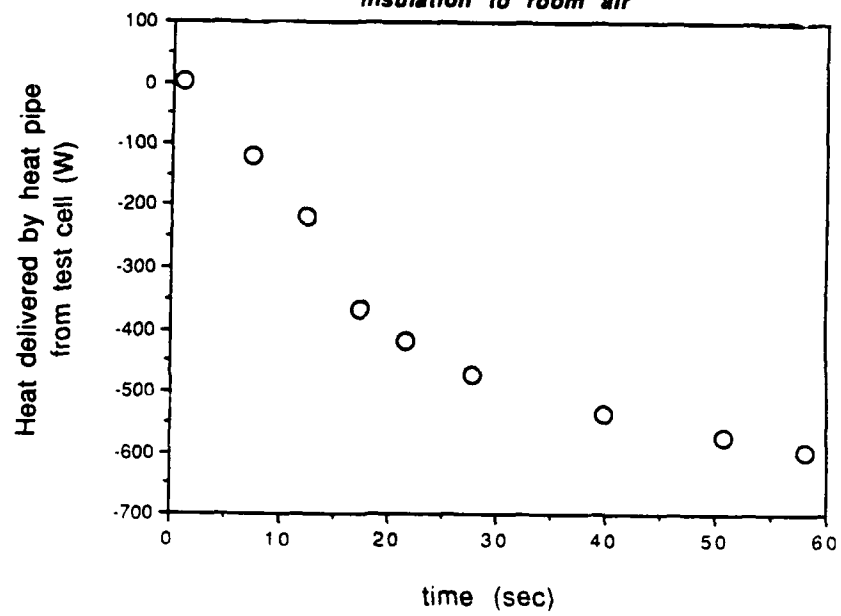
Figure 5.7b: Axial Surface Temperature

INSULATION TO ROOM AIR

□ at 1"   + at 3"   ◇ at 5"   × at 9"
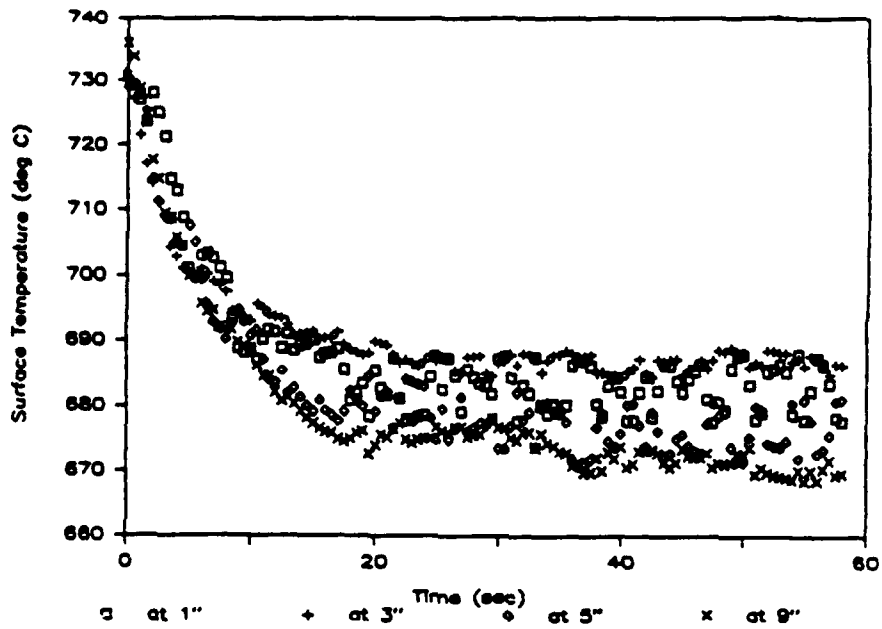
Figure 5.7c: Circumferential Surface Temperature

INSULATION TO ROOM AIR

□ at top   + at right   ◇ at bottom   ▲ at left

54
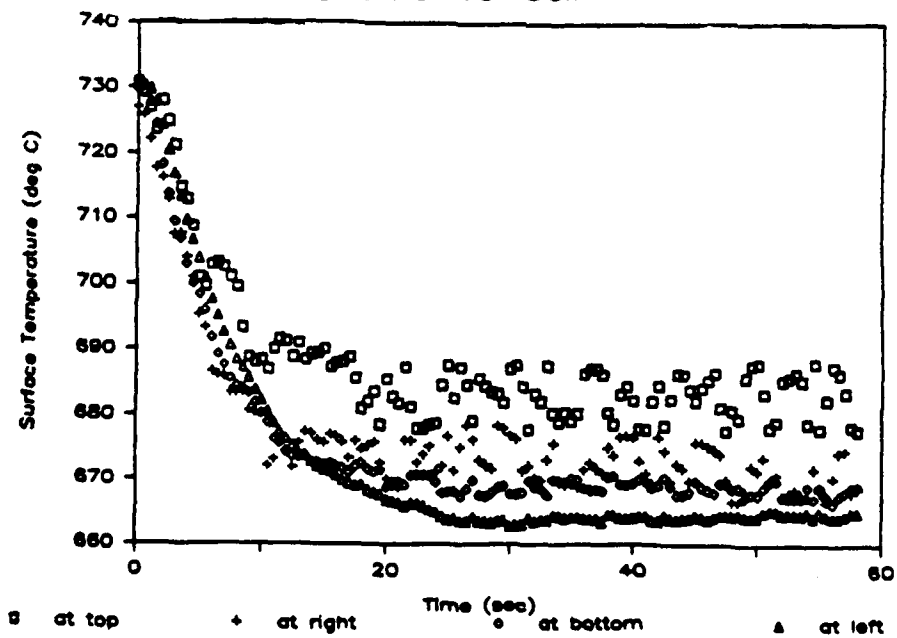
produced different local heat transfer coefficients.

Figures 5.8a, 5.8b, and 5.8c present the results of forward pulsed heat load applied to the condenser. The heat pipe did reverse its heat transporting direction. The time of reversal was about 15 seconds. At the end of this experimental run, the heat pipe was adding about 600 W of heat to the loop; although the steady-state had not been reached, this amount was nearly the net power input from the radiant heater (690 W). The surface temperatures were distributed over a wide range due to the nonuniform temperature distribution in the heater.

The results from loading condition 3 were graphically summarized in Figures 5.9a, 5.9b and 5.9c. Again, Figure 5.91a shows that heat pipe is capable of reversing its operation under this loading condition. The time of reversal was also 15 seconds. From Figures 5.8b and 5.9b, the condenser average temperature increased (or decreased) about 120°C during reversal.

Since the heater added heat to the heat pipe in loading condition 2 at almost the same rate as it removed heat in loading condition 1 (see Figures 5.7a, 5.8a), the 15 second interval seemed to be the time needed for 600 W of heating (or cooling) to raise (or drop) the condenser temperature by 120°C.

Thus, the reversal time is a function of heat pipe properties, heat transfer coefficient and heating conditions, and may range from 15 to 25 seconds.

Figures 5.10a, 5.10b, 5.10c show the heat pipe response when half of the condenser section was heated. Under this heating condition, the heat pipe was still able to remove about 200 W of heat from the test cell. Since heat was also added at the end section of the condenser, the heat pipe must be operating in two directions simultaneously with the condenser section in between two evaporator sections. The surface temperature at the unheated

55

Figure 5.8a: Heat pipe transient response
Room air to full heater
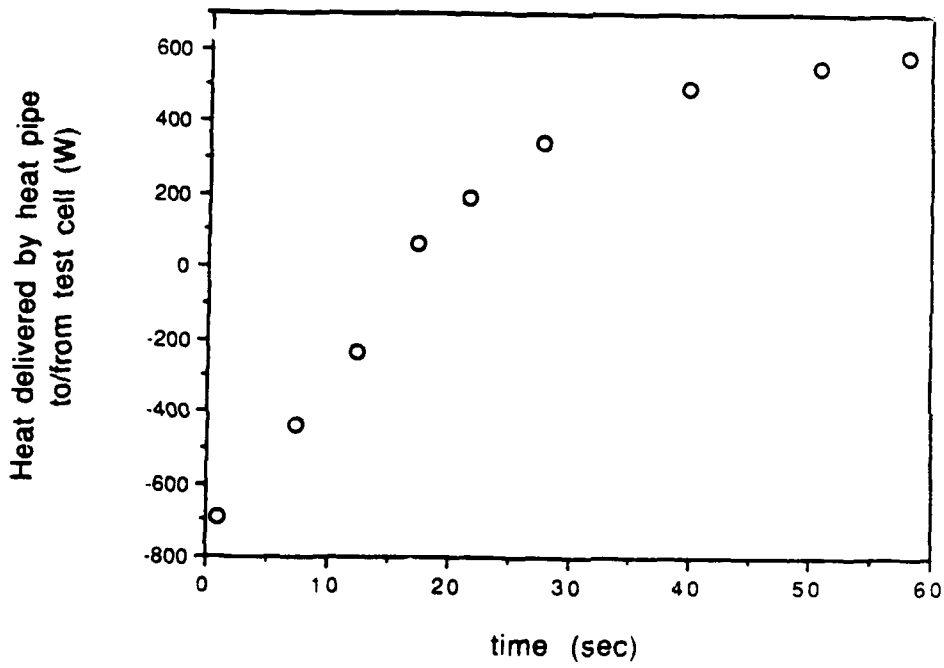
Figure 5.8b: Axial Surface Temperature

ROOM AIR TO FULL HEATER

□ at 1" + at 3" ◇ at 5" x at 9"
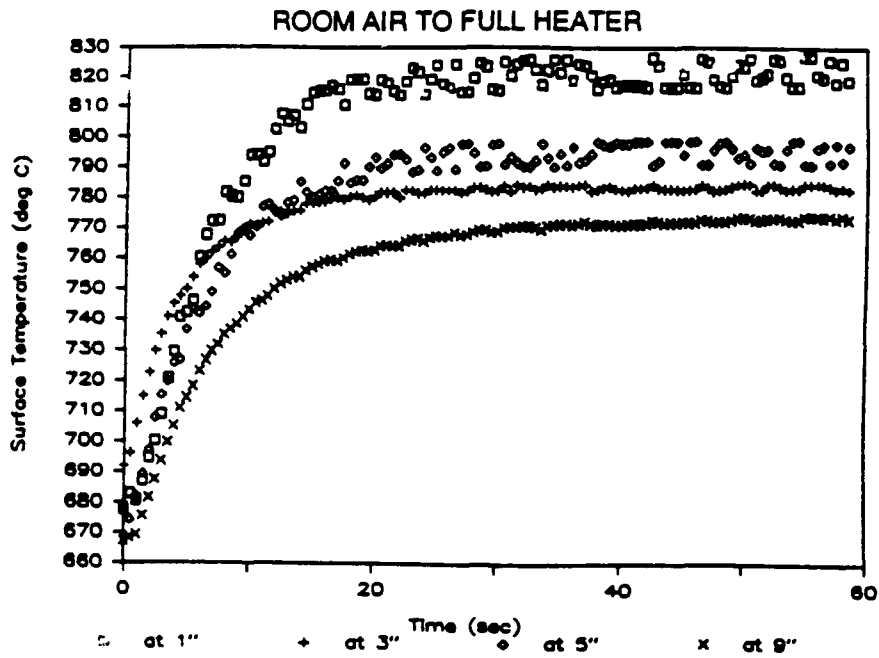
Figure 5.8c: Circumferential Surface Temperature

ROOM AIR TO FULL HEATER

□ at top + at right ◇ at bottom ▲ at left

57
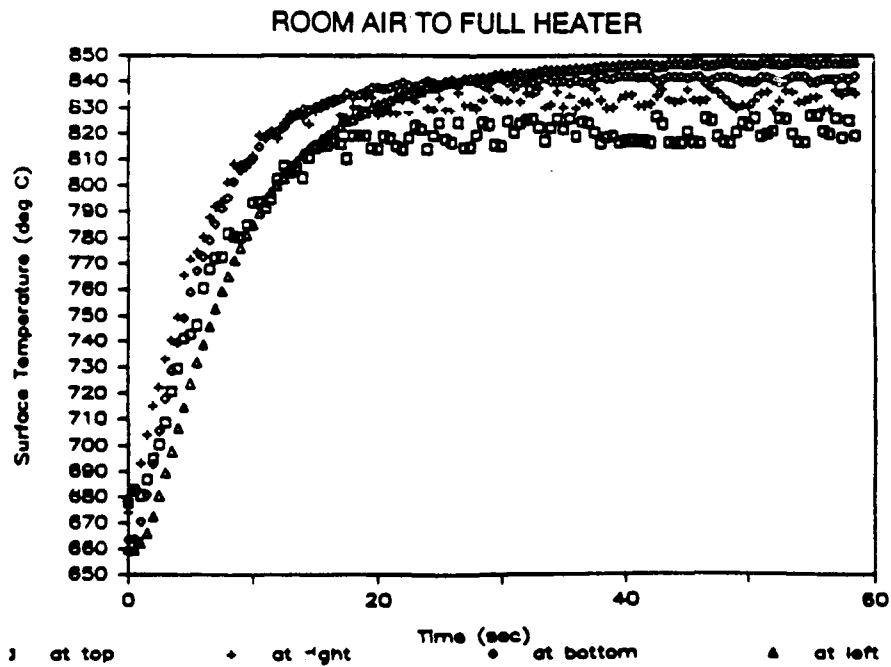
Figure 5.9a: Heat pipe transient response
Full heater to room air
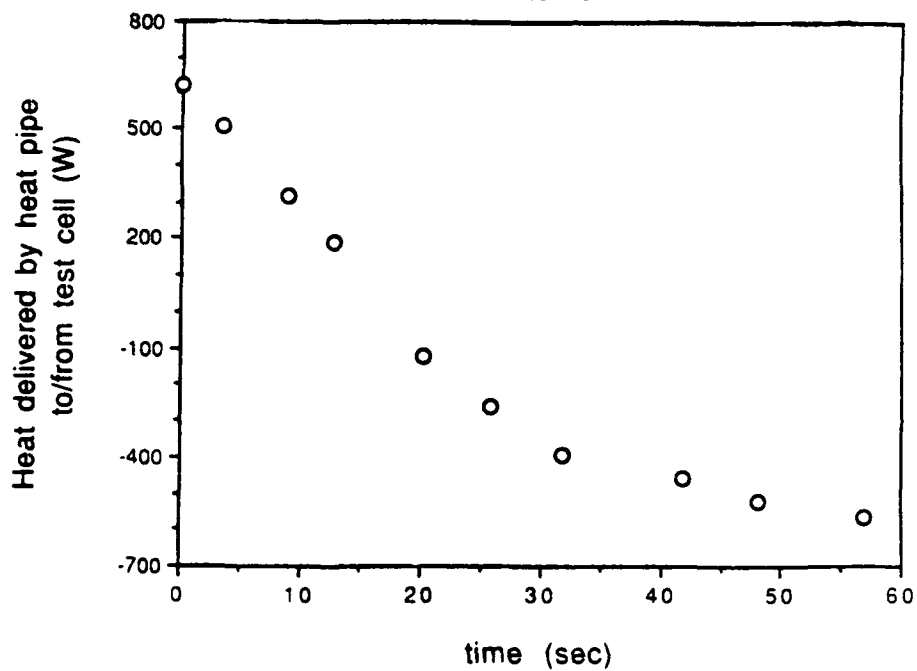
Figure 5.9b: Axial Surface Temperature

FULL HEATER TO ROOM AIR

□ at 1"   + at 3"   ◊ at 5"   x at 9"
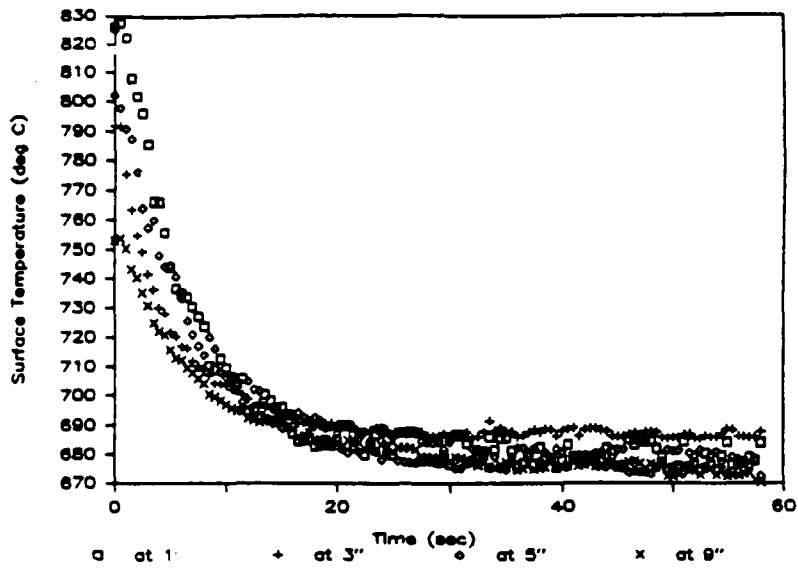
Figure 5.9c: Circumferential Surface Temperature

FULL HEATER TO ROOM AIR

□ at top   + at right   ◊ at bottom   ▲ at left

59
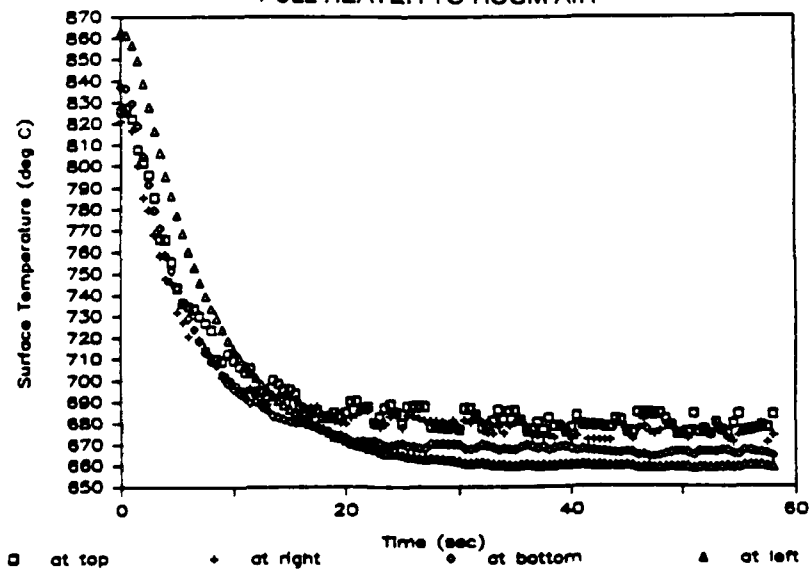
Figure 5.10a: Heat pipe transient response

Room air to 1/2 heater
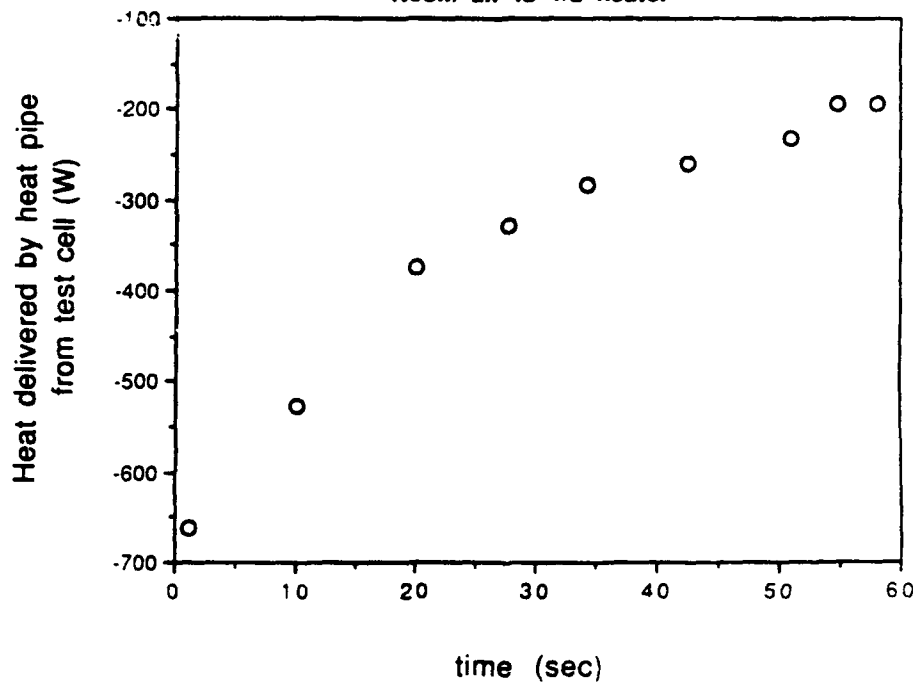
Figure 5.10b: Axial Surface Temperature

ROOM AIR TO 1/2 HEATER

□ at 1" + at 3" ◇ at 5" × at 9"
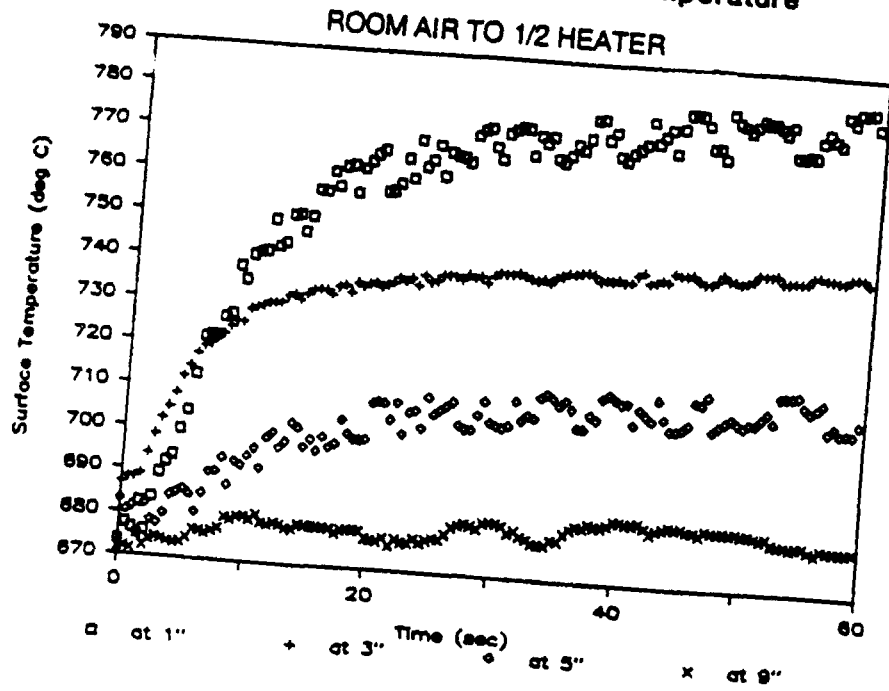
Figure 5.10c: Circumferential Surface Temperature

ROOM AIR TO 1/2 HEATER

□ at top + at right ◇ at bottom ▲ at left

61
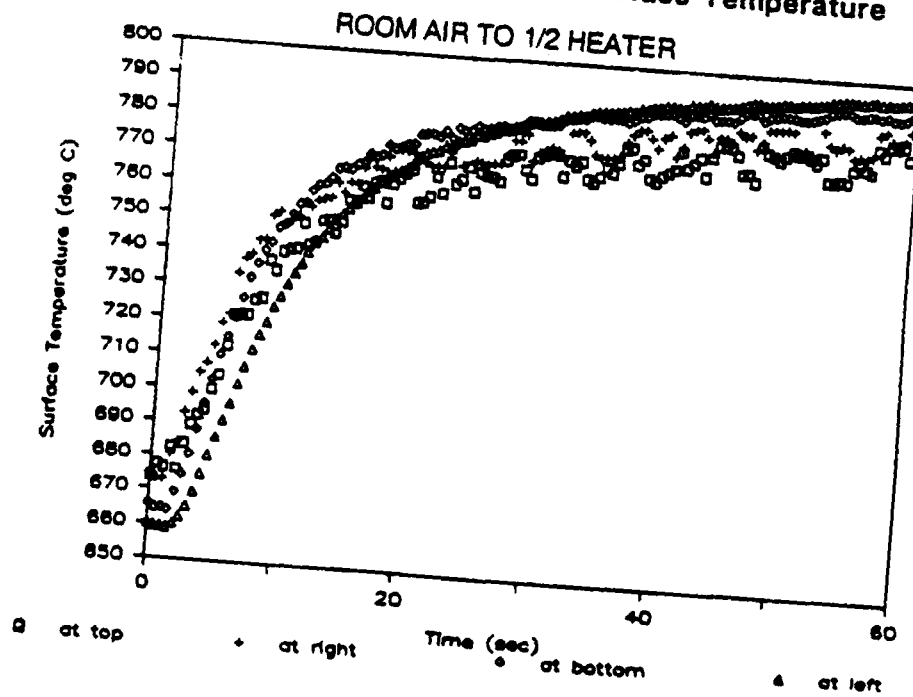
section increased somewhat; however, it remained much lower than the heated section. Moreover, the surface temperature at the unheated section (at 9 inches) oscillated. This was probably due to the flow of vapor, at different temperatures, from both directions toward the cooler middle section. However, when the middle section was insulated (loading condition 5), the heat pipe reversed as seen in Figures 5.11a, 5.11b and 5.11c. While applying condition 5, the radiant heater power was reduced due to the over heating of the heater. Thus the temperature profiles shows a slight decrease.

The axial surface temperatures of condenser during initial start up (from frozen state) was plotted versus time in Figure 5.12. This initial start up was the result of heating up the sodium loop. The thermocouple at the 9 inch location showed a interesting behavior that, however, was not understood. As seen from Figure 5.12, the process was slow. However, during start up process, at least part of the heat pipe was active. The active region extended gradually toward the end of the condenser until all working fluid was molten. The average velocity of this liquid-solid front was approximately 0.036 inch/sec.

The response of heat pipe to high cooling rate at the condenser was also investigated. The results are shown in Figures 5.13a, b, c. Since the compressed air was flowing axially from the end of the condenser, the temperature profile in Figure 5.13b was expected. Except for the themocouple at 1 inch, all other axial temperatures dropped with the same rate up to 25 seconds; they then began to separate starting with the one closest to the condenser end. After 140 seconds, only temperature at the 9 inch location remained above melting temperature. The thermocouple at the 1 inch position showed the fastest cooling rate. However, that thermocouple may not show the true heat pipe temperature since it has the largest surface area and thus subjected to faster cooling. Since the other thermocouples had much smaller

62

Figure 5.11a: Heat pipe transient reponse

room air to 1/2 insulation & 1/2 heater
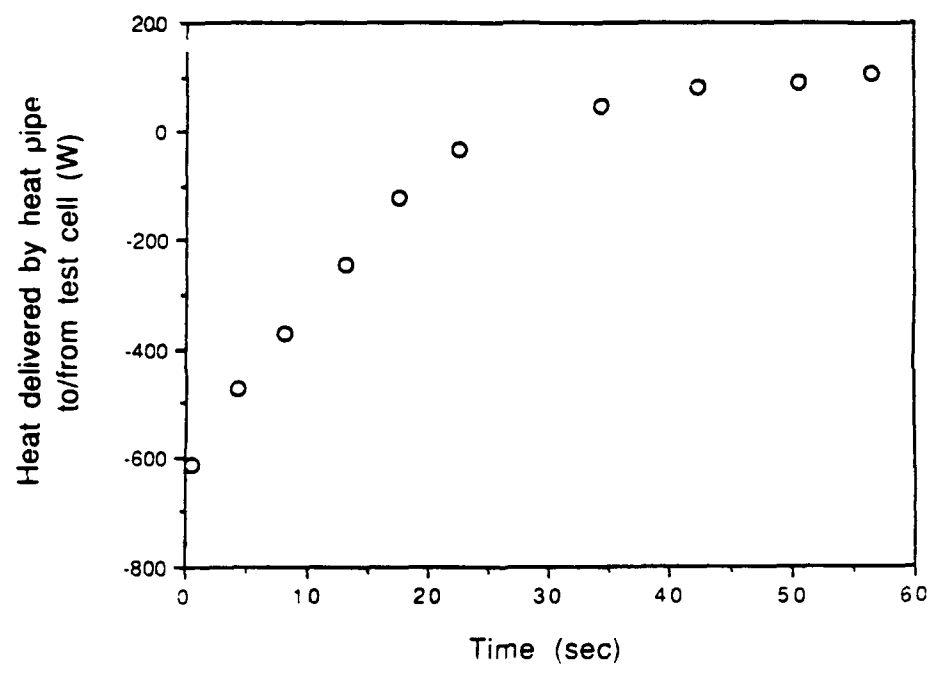
Figure 5.11b: Axial Surface Temperature

ROOM AIR TO 1/2 INSULATION & 1/2 HEATER

□ at 1"   + at 3"   ◇ at 5"   × at 9"
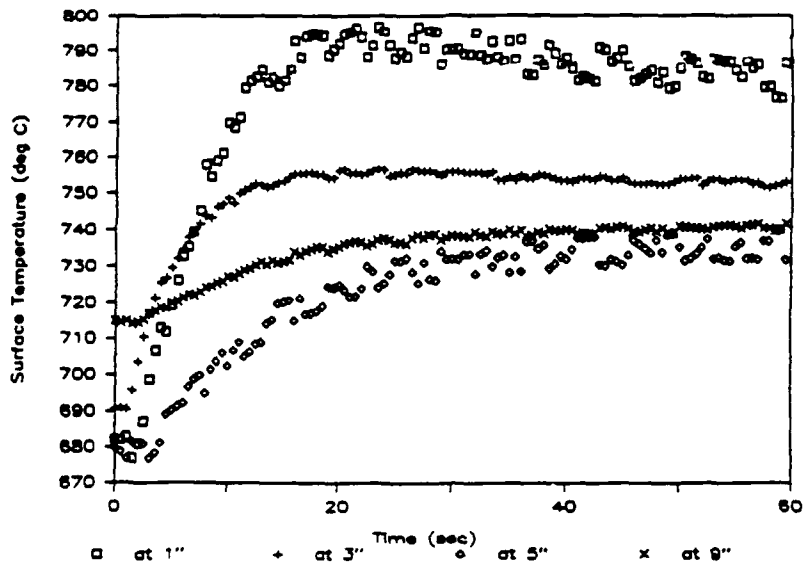
Figure 5.11c: Circumferential Surface Temperature

ROOM AIR TO 1/2 INSULATION & 1/2 HEATER

□ at top   + at right   ◇ at bottom   ▲ at left
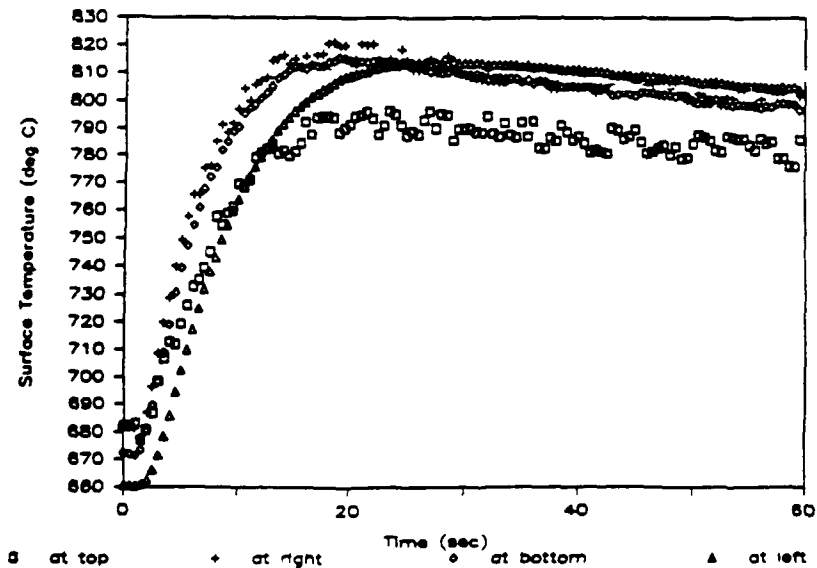
Figure 5.12

Heat Pipe during Start-up

SURFACE TEMP @ VARIOUS AXIAL LOCATIONS

o at 1"　　　+ at 3"　　　◊ at 5"　　　△ at 7"　　　× at 9"
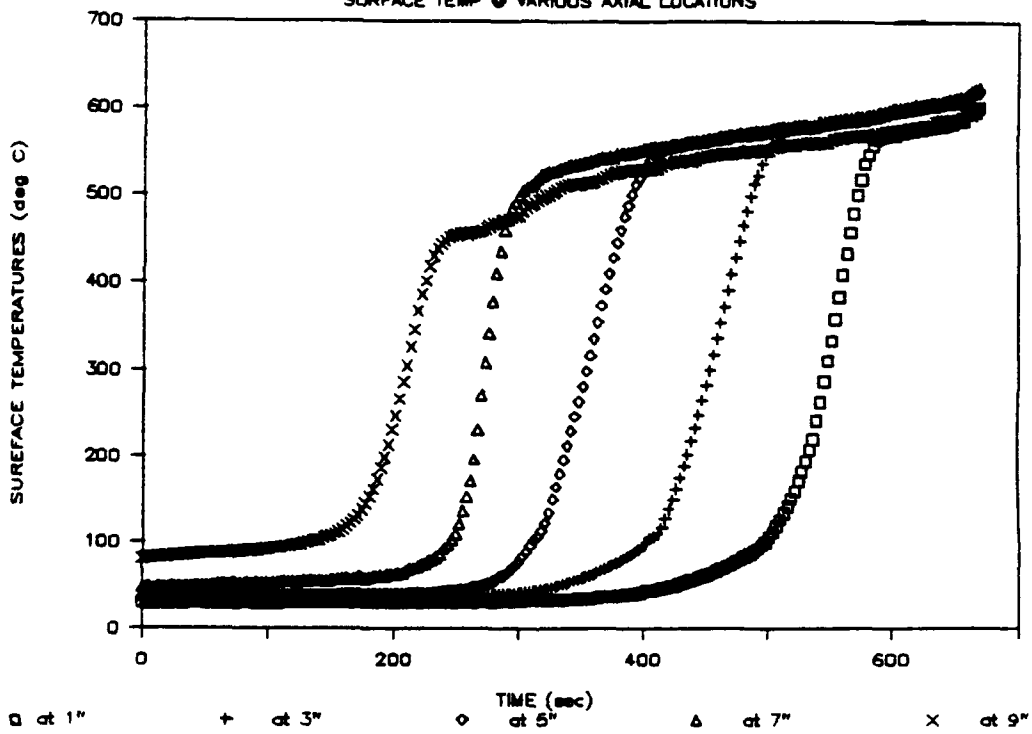
Figure 5.13a: Heat Pipe Transient Response

room air to forced air
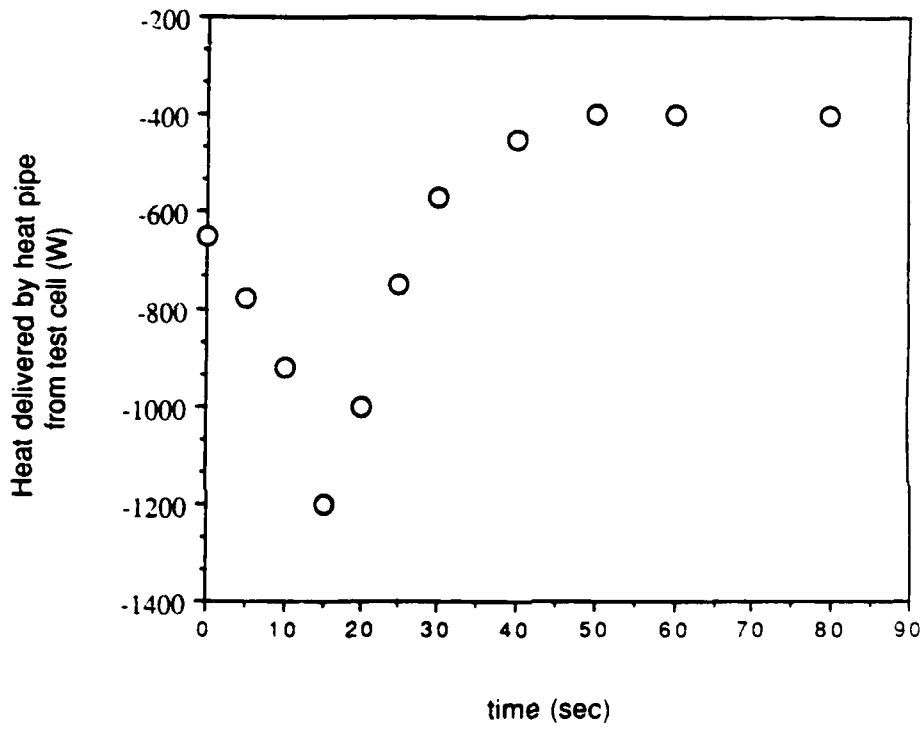
Figure 5.13b: Axial Surface Temperature

ROOM AIR TO FORCED AIR

□ at 1"   + at 3"   ◇ at 5"   △ at 7"   × at 9"
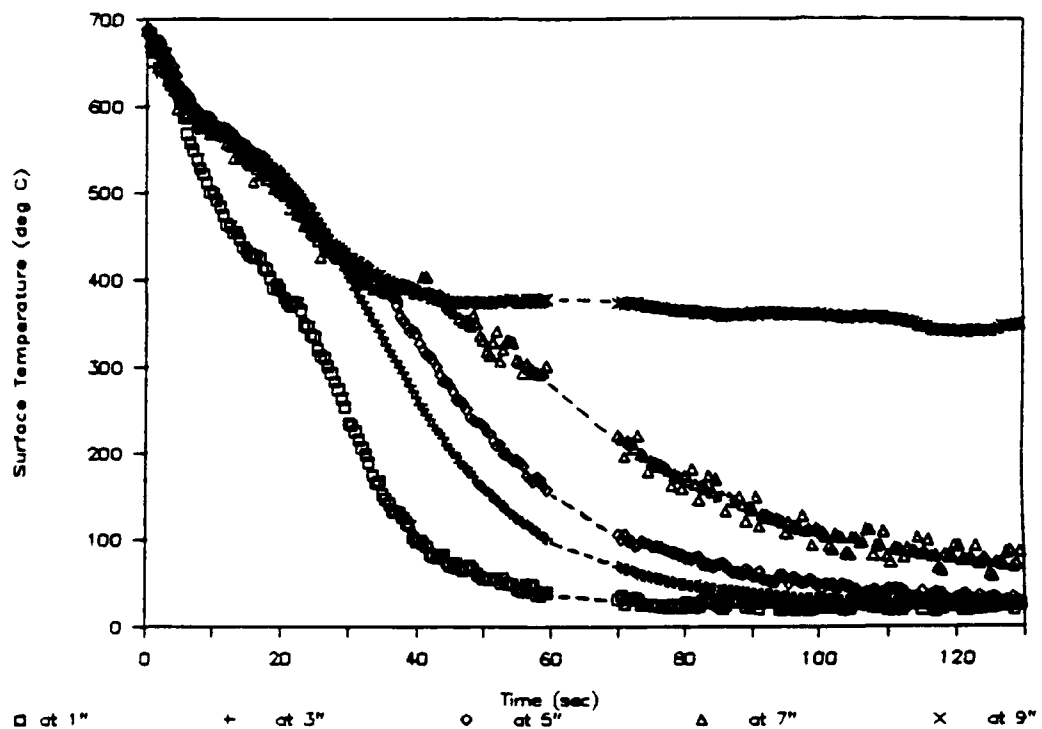
Figure 5.13c: Circumferential Surface Temperature

ROOM AIR TO FORCED AIR

☐ at top   +   at right   ◇ at bottom   △   at left
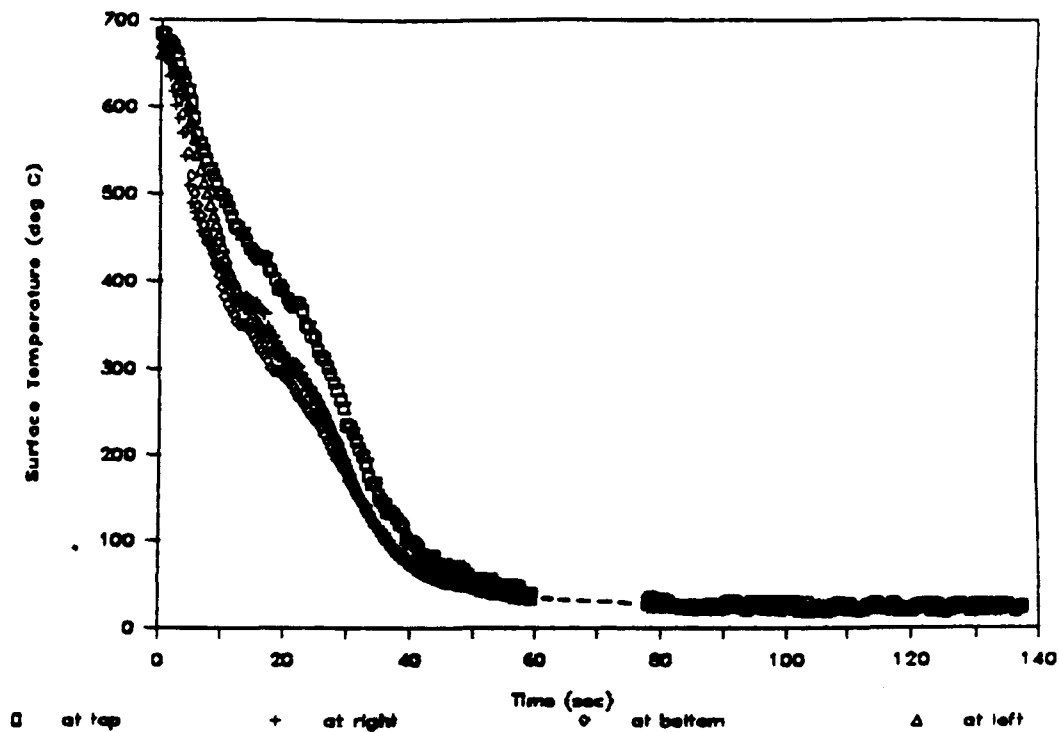
dimension, they were installed beneath the larger one. Consequently, they less subjected to the cooling and tend to show the true heat pipe temperature.

Figure 5.13a illustrates the heat delivered by heat pipe while under forced convection at the condenser. Initially the heat pipe was operating below its maximum heat transport limit. Thus, when the heat transfer condition at the condenser was enhanced, the heat pipe delivered more heat as seen during the first 12 seconds. The heat removal rate peaked at 1200W and started to decrease as time progressed. At the end of the test only 400W of heat was delivered by the heat pipe. At 12 seconds, the heat pipe condenser average temperature was approximately 850 K. From Figure 5.6, the sonic limit of heat pipe is approximately 1000W at 850K. Consequently, the 1200W seem to be the sonic limit of the heat pipe at the experimental conditions.

From the above condition (frozen condenser), the condenser was re-exposed to room air; the results are shown in Figures 5.14a, b. The surface temperature profiles along condenser were similar to those during normal start-up. The solid-liquid front, however, propagated slightly faster at 0.040 inch/sec. This was due to higher loop sodium temperature (1000K); thus, higher evaporator temperature. When forced air was removed, the heat transfer decreased slightly to about 300W. This can be explained by the fact that during forced convection, conduction along the heat pipe controlled the heat transfer rate. When compressed air was removed, the free convection at condenser surface became the factor that dictated the heat removal rate. As sections of the condenser became active, the heat transfer increased.

Figure 5.14a: Heat pipe transient response
forced air to room air
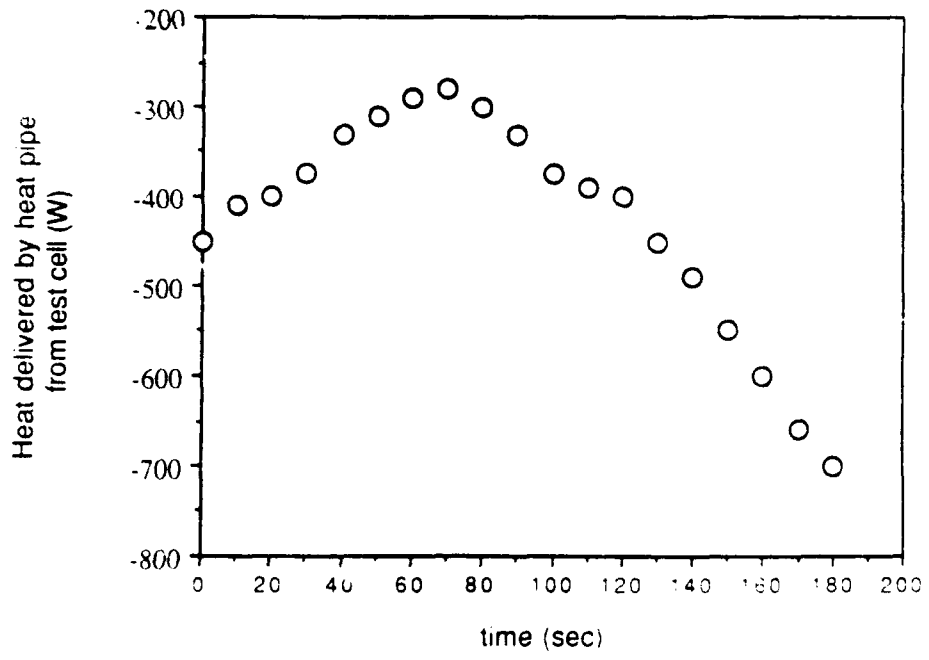
Figure 2.14b
Axial Surface Temperature
FORCE AIR TO ROOM AIR

Plot axes: Surface Temperature (deg C) vs Time (sec)

Legend: □ at 1"   + at 3"   ◇ at 5"   △ at 7"   × at 9"
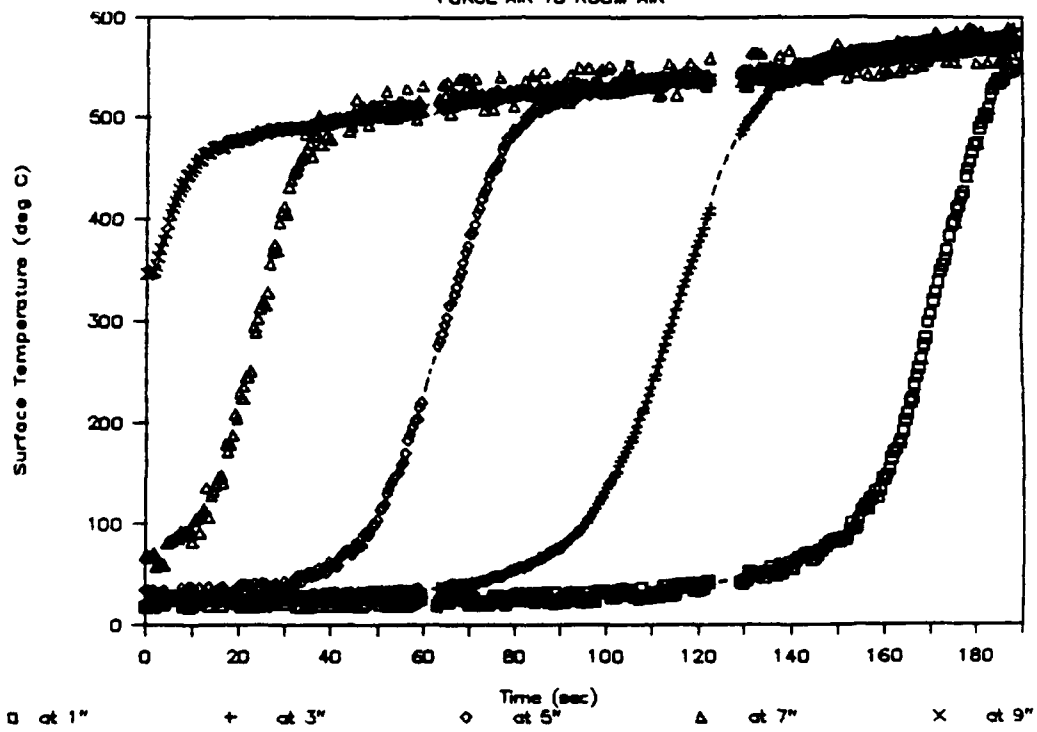
5.4 CONCLUSIONS AND RECOMMENDATIONS

The following can be concluded from the study:

1. Both forward and reverse pulsed heat load applied at the condenser section of a heat pipe can cause the heat pipe to reverse.

2. The time of the reversal is dependent on the heat transfer coefficient, heating conditions and heat pipe properties.

3. The reversal seems to occur at the moment when surface temperature rise (or fall) begins to flatten out.

4. If only the end part of the condenser was heated, the resulting process depends on the heat rejection rate at the unheated section. The heat pipe will function in both directions simultaneously provided that the unheated middle section is able to remove heat being input from both ends. When the middle unheated section fails to remove all the heat input, the heat pipe will reverse.

5. During start-up, part of the heat pipe is active. The active region extends slowly as the liquid-solid front moves to the end of the condenser.

6. The heat pipe does exhibit a limit on heat transport. This limit is a strong function of temperature.

There were two other thermal loading conditions that were not studied in this experiment. One involves the heating of a section of the condenser that is next to the evaporator. The other is the high intensity heating at a small area on the condenser surface. A current radiant heater, due to its dimension, could not be used to provide these type of thermal loadings.

It is believed that the transient response of heat pipe is dependent on heat transfer characteristics at the condenser surface, evaporator surface and within the heat pipe itself. In this research only the conditions at condenser surface were studied. The heat pipe response to conditions at evaporator

72

surface can be studied by changing the sodium loop flow rate and temperature. When the modification of the test cell is needed for testing of other heat pipes, it is recommended that the new test cell must provide: a) sufficient surface area for the evaporator, and b) spiral flow characteristics to enhance the heat transfer.

REFERENCES

1.   Tilton, D.E., Chow, L.C., and Mahefkey, E.T., "Transient Response of a Liquid
      Metal Heat Pipe", Journal of Thermophysics and Heat Transfer, Vol. 2, No 1,
      pp. 25-30.

2.   Tilton, D.E. Chow, L.C., and Mahefkey, E.T., "A Two-Dimensional Transient
      Liquid Metal Heat Pipe Model", AIAA Paper 88-2681, June 1988.

3.   Chi, S.W., Heat Pipe Theory and Practice, Hemisphere Publishing Corp.,
      Washington, 1976.

4.   Colwell, G.T. and Chang, W.S., "Measurement of Transient Behavior of a
      Capillary Structure under Heavy Thermal Loading," International Journal of
      Heat and Mass Transfer, Vol. 27, No. 4, 1984 pp, 541-50

5.   Chow, L.C. and Zchong, J., "Analysis of Heat Pipe Start-up From the Frozen
      State," AIAA Paper 90-1786, June 1990.

6.   Foust, O.J., "Liquid Metal Handbook: Sodium and NaK Supplement," US
      Atomic Energy Commission, June 1967.

7.   Holman, J.P., Experimental Methods for Engineers, McGraw Hill, Inc., 1978.

8.   Krietz, P.K., Design and Construction of Liquid Metal Heat Transfer Facility,
      Thesis, University of Kentucky, 1989.

APPENDIX A

START-UP AND OPERATIONAL PROCEDURES

This start-up procedure is written with the assumption that the personnel involved are thoroughly familiar with the sodium loop. A schematic of control cabinet is shown in Figure A.1.1. The sodium is initially left in lines, surge tank and cold trap. Only a minimum amount of sodium is remained in the dump tank. All valves to dump tank are closed. Cold trap valves are also closed. By-pass valve is opened.

<u>Preliminaries</u>

-Turn on system power.

-Set pump flow sensor low limit to 0 mV, thus override the sensor.

-Set loop ambient temperature sensor to 80°C.

-Check temperature instrumentation.

-Check level and flow instrumentation, turn amplifiers on.

-Check for cover gas leaks and set pressure at 3 psig.

-Check CO_2 system.

-Check or close 2 valves to dump tank.

-Check or close 2 cold trap valves.

-Check or open by-pass valve near pump.

-Start scrubber system - Fan and pump.

-Close the sodium loop housing.

-Open and close exhaust fan valve to check air flow and systems negative pressure in the loop.

-Close exhaust fan valve
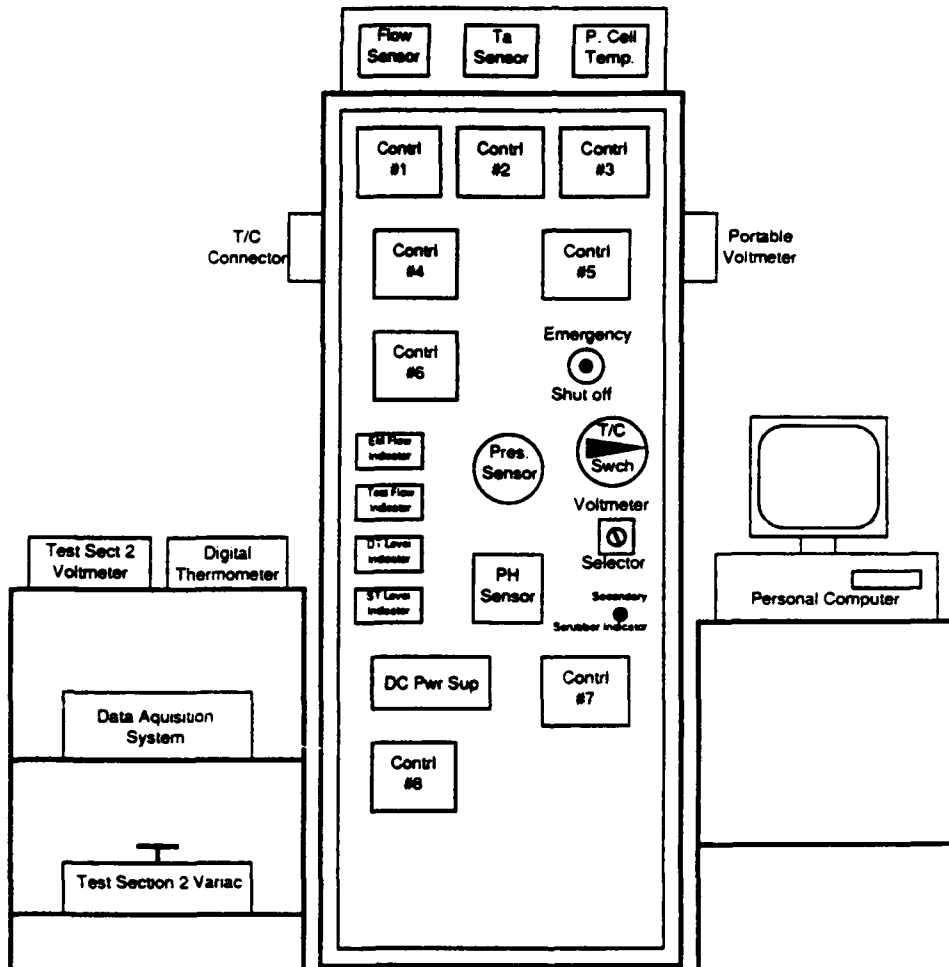
Figure A.1.1: Sodium Loop Control Instrumentation Cabinet

Heat up of loop

Notes: - sodium boils at 881°C (1618°F)

- Heater fails at about 1100°C (2012°F)

- Control point of thermocouple in heat up is 80 to 150°C cooler than heater.

- 150V on the 220V heater reaches about 920°C (1688°F) without cooling for single-layer insulated line.

- Maximum temperature for thermocouple control point is 850-880°C (1562-1616°F).

- Loop design limit of stainless steel at 10 psig is 950°C (1742°F).

- Check temperature distribution since fan is running before heating.

- Turn test cell heater switch on.

- Start to heat all systems (Except - line from surge to dump tank, surge tank filling arm, dump tank drain lines, cold trap and its lines, dump tank #2, and frozen section). Use a 10°C temperature request or low voltage (50V) only.

High voltage (160-180V) can be used on the cooler since it was not insulated.

- Check temperature distribution after some increase in temperature. Pay special attention to TC# 17 and #23; they are heater surface temperature.

- Heat the whole system in stages. The whole system should be allowed to reach 149°C (300°F) before any part is intentionally heated higher.

- Heat the whole system to 149°C (300°F).

- Check and close all valves, if necessary.

- Heat the whole system to 205°C (400°F).

- Dump tank should be maintained at 205°C (400°F).

- Heat the whole system except dump tank to 260°C (500°F) and hold.

- Check temperatures for any cold spots. The pump cell temperatures,TC#1,

   #19 and #29, should be cold (about 80°C) since it was not heated.

- If air-Na cooler too hot open fan, leave heater on.

- Monitor level indicators.

- Turn on pump variac and set pump voltage to 100V.

- Heat pump cell slowly using the pump current by:

   a. Turn on pump

   b. Monitor pump cell temperature and flow indicator

   c. If no flow, turn off pump when 10°C rise is reached.

   d. Wait for pump cell temperature to stablize.

   e. Repeat a-d until sodium is flowing or until pump cell reaches 150°C.

- If pump fails to move the sodium, there must be cold spot in loop. Heat the

   whole system, except dump tank, to 316°C (600°F) and repeat a-e until

sodium

   is flowing.

- Open by-pass valve and allow pumping (without heating) for about 5 minutes

   to remove any hot/cold spots.

- Set pump voltage to achieve the desired sodium flow rate. Use test section

   flow meter output and calibration curve (Figure A.1.2) as an estimation.

   Remember that flow rate output is also dependent of temperature.

- Set pump flow sensor low limit to slightly less than the flow meter voltage

   output.

- Turn off test cell heater switch.

Figure A.1.2: CALIBRATIONAL CURVE

for Test Section Flow Meter

Plot of Sodium Flow Rate (g/sec) versus Output Voltage (mV). Legend: ○ at 730°C test cell temperature.

$$\dot{m} = 2.3041 + 72.4 \ (mV)$$
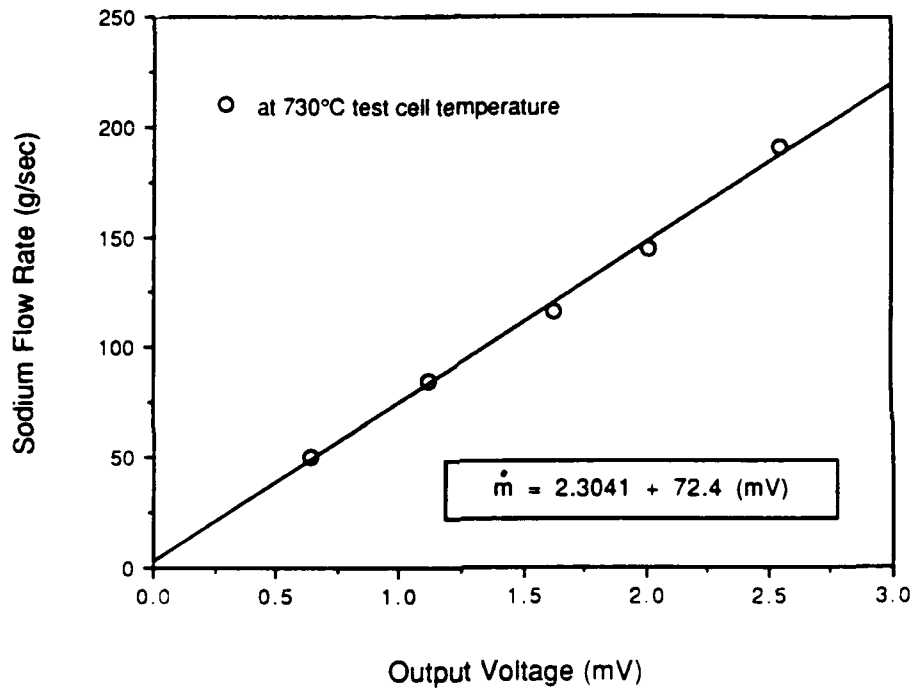
- Start heat up loop to higher temperature

. Higher voltage (150-200V) can now
be used.

- Watch by-pass valve and pump cell temperature. Exhaust fan valve and
cooler heater voltage can be adjusted to control pump and by-pass valve
temperatures. Maximum temperature for pump cell and by-pass valve is
650°C (1200°F).

- Continue heating up loop until desired test cell temperature is reached. Note
that set point temperature must be higher than the actual temperature to have
any voltage output. Thus to compensate for heat losses, it is necessary to
over-set the controller.

Shut system down

- Turn off all heaters.

- Increase/decrease pump voltage to 100V

- Open exhaust fan valve fully.

- Allow pumping until pump cell temperature drops to 100°C (212°F).

- Turn off pump.

- Turn off pump variac.

- Turn off system power.

- Set cover gas pressure to 5 psig.

- Turn off scrubber system.

Emergency Shut Down

- Hit emergency button.

- Open cover gas pressure relief valve.

- Open exhaust fan valve.

- If fire, open carbon dioxide valve.
- Monitor temperature in enclosure.

APPENDIX B

SODIUM FLOW CALIBRATION PROCEDURES:

As stated in the section describing the electromagnetic flow meter, there are many factors that affect the flow meter output. These factors include the temperature and time dependence of the permanent magnet, the shunting effect of wall and the end regions, and the thermal emf. Due to these factors, it is impossible to establish one single calibrational curve. The sodium flow rate must be determined every time the loop is running. While the flow meter serves as an indication of how much sodium is flowing, a method must be developed to determine the actual flow rate. This method utilizes the principle of energy conservation at the test section 2 of loop where heater power, inlet and outlet temperatures are monitored. Figure B.1 shows the setup for flow rate calibration. Four high-sensitive thermocouples were attached to the stainless steel pipe by hose clamps, two at the inlet and two at the outlet. The inlet and outlet temperatures are the average of each two thermocouples. The power input is determined by measuring the electrical voltage and current into the test section 2 heater. The steady state energy balance (Figure B.2) of that section gives:

$$Q_{in} = m \, C_p \, (T_o - T_i) + Q_{loss} \qquad (3)$$

Where Q_{in} is the heater electrical power input (equals the product of input voltage and current), Q_{loss} is the total heat loss to the surrounding from that section, m is the sodium mass flow rate, C_p is the specific heat of sodium, T_o and T_i are outlet and inlet temperatures, respectively. If heat loss is assumed to be constant, then the plot of Q_{in} vs. $C_p(T_o - T_i)$ is a straight line whose slope is
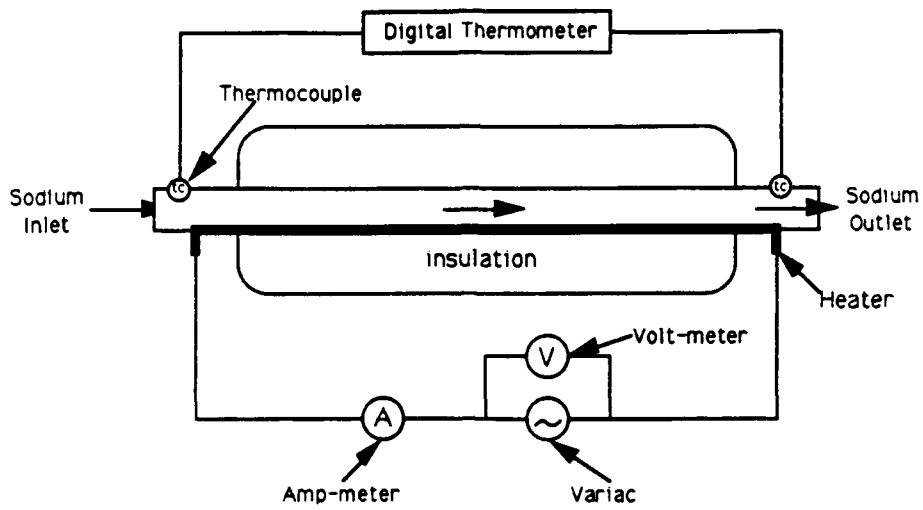
Figure B. 1: Schematic of Set-up at Test
Section II for Flow Calibration
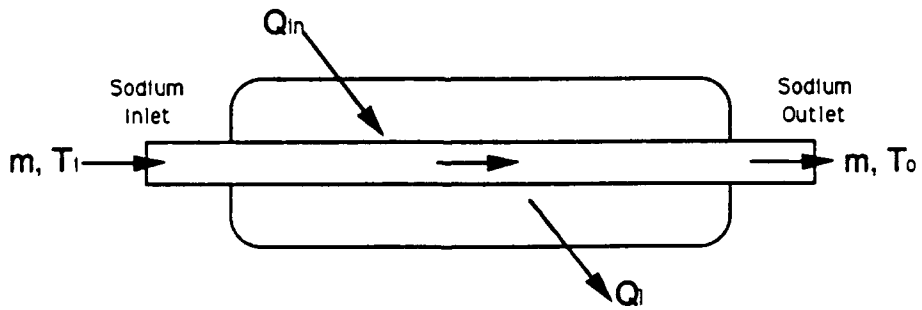
Figure B. 2: Energy Balance at Test Section II

the mass flow rate and y-intercept is the heat loss. Since the heat loss is dependent of temperature, this assumption requires that the heat input is neither too large nor too small so that the average temperature of sodium remains relatively constant over the the range of input power.

PROCEDURES:

The inlet and outlet temperatures can be read from FLUKE digital thermometer channels 0 and 2, respectively. The current can be measured using clamp-on ammeter; and the voltage can be read from voltmeter.

- Record Test section flow meter output. It is necessary to occasionally adjust
  the pump voltage to maintain the same flow since pump voltage varies slightly.
- Heat up loop to desired test temperature if necessary.
- Allow loop to reach steady state and record inlet and outlet temperatures,
  voltage and current. These are reference data.
- Base on reference data, set voltage so that $(T_o - T_i)$ is between 0 and 15°C.
- Allow loop to reach steady state and then record the data. Note: the current
  must be measured from both leads and the averaged value will be used.
- Repeat to obtain about 4-5 sets of data.

FLOW RATE CALCULATION:

- Calculate the power input ($Q = V\,I$) and $C_p\,(T_o - T_i)$ for each set of data points.
- Use linear regression to determine the flow rate, i.e., the slope of the best fit
  line of Q_{in} vs. $C_p\,(T_o - T_i)$. The regression coefficient must be better than 0.98;
 otherwise repeat the calibration.

84

APPENDIX C

STEADY STATE HEAT LOSS FROM LOOP PIPING

A segment of the piping was constructed to the exact dimension of the loop piping (include heater, shim stock, insulation, and aluminium tape). Two thermocouples were installed $180^{\circ}C$ apart, one measured heater temperature and the other simulated the control temperature. Two sets of experiments, one for single insulation and one for double insulation, were carried out in room air $(25^{\circ}C)$ to determine the steady-state heat loss from loop piping. Electrical power was supplied to the heater; then the system was allowed to reach steady-state. At steady-state, heat loss is the input power. Figures C.1 and C.2 show the results.

Figure A.3.1: Steady State Heat Loss
for Double Insulation
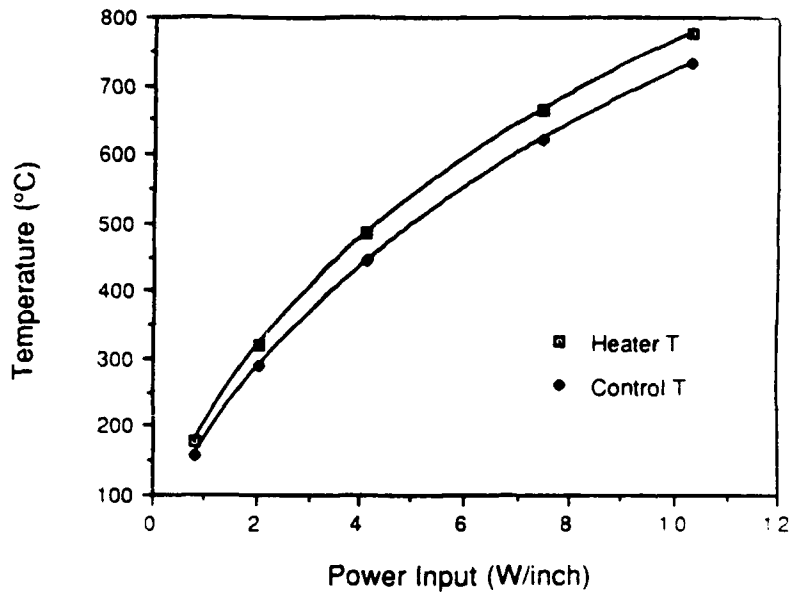
Figure A.3.2: Steady State Heat Loss
for Single Insulation
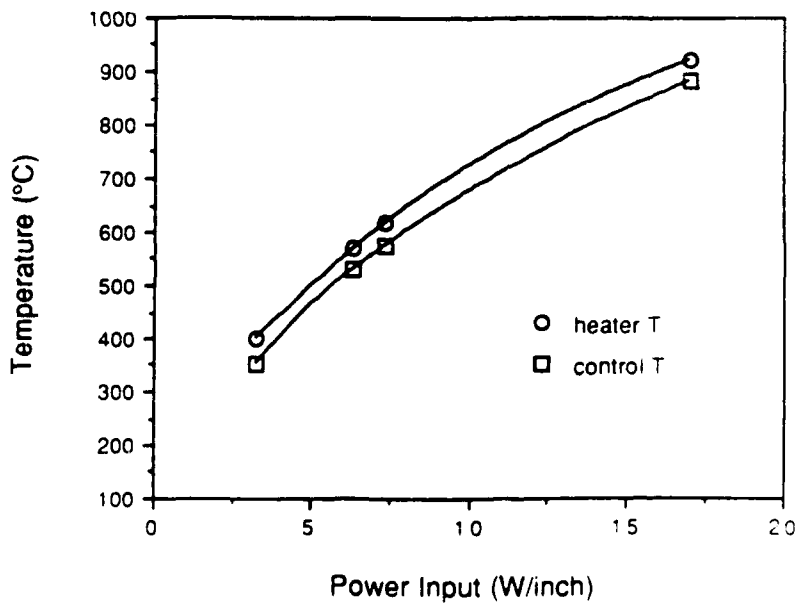
APPENDIX D

HEAT TRANSPORT LIMIT OF HEAT PIPE

The sonic, entrainment, and capillary limits of the heat pipe used in the experiment were calculated at various temperatures and listed in table D.1.

Table D.1 Heat Transport Limit of Heat Pipe*

Temp. (K)	Q sonic (W)	Q entrain (W)	Q capillary (W)
427	0		
506	0		
558	0		
621	3		
702	26		
807	237		
897	1121		
900	1161	1468	
946	2180	1943	
1000		2417	3034
1035		3072	2946
1100			2781
1173			2619
1273			2438
1350			2044

*missing data are larger in magnitude than the values shown at given temperature.